Received: 15 July 2022 | Revised: 31 October 2022 | Accepted: 30 December 2022

DOI: 10.1002/jnr.25167

RESEARCH ARTICLE

JOURNAL OF Neuroscience Research

The association of astrogliosis and microglial activation with aging and Alzheimer's disease pathology in the chimpanzee brain

Melissa K. Edler[1] | Emily L. Munger[1] | Hannah Maycon[1] | William D. Hopkins[2] | Patrick R. Hof[3] | Chet C. Sherwood[4] | Mary Ann Raghanti[1]

[1]Department of Anthropology, School of Biomedical Sciences, and Brain Health Research Institute, Kent State University, Kent, Ohio, USA

[2]Department of Comparative Medicine, University of Texas MD Anderson Cancer Center, Bastrop, Texas, USA

[3]Nash Family Department of Neuroscience and Friedman Brain Institute, Icahn School of Medicine at Mount Sinai, New York, New York, USA

[4]Department of Anthropology and Center for the Advanced Study of Human Paleobiology, The George Washington University, Washington, District of Columbia, USA

Correspondence
Melissa K. Edler, Department of Anthropology, School of Biomedical Sciences, and Brain Health Research Institute, Kent State University, 750 Hilltop Drive, Kent, OH 44242, USA.
Email: medler@kent.edu

Funding information
National Institutes of Health, Grant/Award Number: NIH 3U42OD011197-19S1, NIH R01AG067419-01A1, AG014308 and NS092988; National Science Foundation, Grant/Award Number: NSF BCS-1846201; NINDS, Grant/Award Number: NS0-73134 and NS-402867

Abstract

Aging and neurodegenerative disorders, such as Alzheimer's disease (AD), trigger an immune response known as glial activation in the brain. Recent evidence indicates species differences in inflammatory responses to AD pathology, highlighting the need for additional comparative studies to further understand human-specific neuropathologies. In the present study, we report on the occurrence of astrogliosis, microglial activation, and their relationship with age and AD-like pathology in a cohort of male and female chimpanzees (*Pan troglodytes*). Chimpanzees with severe astrogliosis exhibited widespread upregulation of hypertrophic astrocytes immunoreactive for glial fibrillary acidic protein (GFAP) throughout all layers of the dorsolateral prefrontal cortex and a loss of the interlaminar palisade. In addition, extreme astrogliosis was associated with increased astrocyte density in the absence of significant microglial activation and AD lesions. A shift from decreased resting to increased phagocytotic microglia occurred with aging, although proliferation was absent and no changes in astrogliosis was observed. Vascular amyloid correlated with decreased astrocyte and microglia densities, while tau lesions were associated with morphological changes in microglia and greater total glia density and glia: neuron ratio. These results further our understanding of inflammatory processes within the chimpanzee brain and provide comparative data to improve our understanding of human aging and neuropathological processes.

KEYWORDS
aging, Alzheimer's disease, astrocyte, astrogliosis, chimpanzee, microglia, neuroinflammation, nonhuman primate, RRID:AB_90949, RRID:AB_839504, RRID:AB_223647, RRID:AB_2109645, RRID:AB_2190927, RRID:AB_2564657

Emily L. Munger and Melissa K. Edler should be considered joint first authors.

Edited by Junie Paula Warrington and Stephen J. Crocker. Reviewed by John Zhou and Larry S. Sherman.

1 | INTRODUCTION

Astrocytes and microglia play an important role in the brain's immune system and undergo an activation process in response to aging and neurodegenerative diseases, such as Alzheimer's disease (AD) (Kettenmann et al., 2011; Sofroniew & Vinters, 2010). Astrogliosis and microglial activation are defined by a spectrum of molecular, cellular, and functional changes that correspond to the severity and progression of the underlying condition (Heneka et al., 2010; Kettenmann et al., 2011; Sofroniew & Vinters, 2010). Astrogliosis results in upregulation of glial fibrillary acidic protein (GFAP) mRNA and protein, hypertrophy of the soma, elongation of dendritic processes, and loss of domain organization (Pekny et al., 2014). Similarly, microglia use highly motile ramified processes to survey the cellular environment in their resting state, but upon activation, they exhibit a phenotypic graded response of decreased arborization, enlarged cell soma, and shortened or total loss of cellular processes (Kettenmann et al., 2011). In addition, activated microglia can proliferate and migrate to a lesion site to provide additional defense and restoration of tissue homeostasis.

During aging, mild astrogliosis with GFAP upregulation occurs in humans (*Homo sapiens*), although overall astrocyte density does not change (Beach et al., 1989; Cotrina & Nedergaard, 2002; Nichols et al., 1993; Pelvig et al., 2008). Conversely, humans display increased microglial activation and density with age in the neocortex, including the hippocampal formation, entorhinal cortex, and white matter (DiPatre & Gelman, 1997; Gefen et al., 2019; Pelvig et al., 2008). When age-associated alterations in glial cells occur, they can produce persistent chronic inflammation, making the brain increasingly susceptible to neurodegenerative processes. Thus, in AD, greater levels of astrogliosis and microglial activation are associated with the characteristic neuropathologic inclusions of amyloid-beta (Aβ) plaques and tau-associated neurofibrillary tangles (NFTs) in the temporal cortex and hippocampus (Ekonomou et al., 2015; Harpin et al., 1990; Hoozemans et al., 2011; Marlatt et al., 2014; McGeer et al., 1987; Serrano-Pozo et al., 2011; Streit et al., 2009).

Whether similar age- and pathology-related changes appear in the brains of closely related nonhuman primates has been examined in a small number of studies. In aged rhesus macaques (*Macaca mulatta*), GFAP expression was greater in the white matter, prefrontal cortex, and hippocampus, although like humans, astrocyte density was not increased compared to young monkeys (Haley et al., 2010; Sloane et al., 2000). Other studies also support a lack of age-related effects on astrocyte density in the fornix, primary visual cortex, frontal lobe, and midbrain of rhesus macaques (Peters et al., 2008, 2011; Robillard et al., 2016). However, astrocytes in older macaques do have a greater number of filaments in their processes and increased number of cellular inclusions. Conversely, the impact of age on microglial activation and density changes in nonhuman primates is inconsistent. Rhesus macaques display age-related increases in total neocortical microglial densities and in microglial expression of the major histocompatibility complex class II (MHCII) protein in subcortical white matter tracts (Robillard et al., 2016; Shobin et al., 2017).

Significance

Aging and Alzheimer's disease (AD) trigger activation of glial cells known as astrocytes and microglia in the brain's immune system. Recent evidence indicates that humans differ from other species in their inflammatory responses to aging and AD pathology, highlighting the need for comparative studies. Here, we report on the occurrence of astrogliosis, microglial activation, and their relationship with age and AD pathology in chimpanzees (*Pan troglodytes*). We also describe an extreme form of astrogliosis in chimpanzees in the absence of significant microglial activation and AD lesions. This study adds to our understanding of neurological differences between species during the aging process.

In addition, the mean average area occupied by MHCII-expressing microglia was greater in mature female pig-tailed macaques (*Macaca nemestrina*) compared to young adult and juveniles (Sheffield & Berman, 1998). In contrast, microglia densities did not change with age in the hippocampus of marmosets (*Callithrix jacchus*), although decreased numbers of resting (nonactivated) microglia were noted for older individuals (Rodriguez-Callejas et al., 2016). Microglia density also was not affected by age in the visual cortex, substantia nigra pars compacta (SNc), and ventral tegmental area of rhesus monkeys (Kanaan et al., 2010; Peters et al., 2008; Rodriguez-Callejas et al., 2016). Furthermore, microglial, astrocyte, and total glia densities did not vary with age in the neocortex and hippocampus of chimpanzees (Edler et al., 2018, 2020; Munger et al., 2019). Together, these data indicate brain regions are differentially impacted by neuroinflammation during the aging process in nonhuman primates.

Only a handful of reports have investigated the neuroinflammatory response to AD pathology in nonhuman primates. Rhesus monkeys exhibit activated microglia and astrocytes concomitant with fibrillar Aβ neuritic plaques, and amyloid precursor protein (APP) deposition occurs intracellularly in astrocytes and microglia near plaques in rhesus, lion-tailed (*Macaca silenus*), and long-tailed macaques (*Macaca fasicularis*) (Härtig et al., 1997; Martin et al., 1994; Robillard et al., 2016). Injection of fibrillar Aβ into the cortex of aged marmosets and rhesus macaques induced tau hyperphosphorylation and microglial recruitment, and a macrophage inhibitor eliminated fibrillar Aβ toxicity in elderly macaques (Geula et al., 1998; Leung et al., 2011). In aged chimpanzees, Aβ-immunoreactive (ir) plaques and vessels as well as tau pathologies were associated with greater glial activation in the neocortex and hippocampus (Edler et al., 2018; Munger et al., 2019). However, to further understand the distinct features of the human brain in relation to aging and disease, additional studies in our closest living relatives are needed.

Here, we build upon our previous work measuring astrogliosis and microglial activation in aged chimpanzees (n = 20, 37–62 years) by adding a group of young chimpanzees (n = 11, 12–27 years) to

better identify neuroinflammatory changes associated with aging. We provide a quantitative analysis of astrocyte, microglia, and overall neuron and glia densities and their correlations with age, sex, and AD-like pathology. In addition, we document the presence of an extreme form of astrogliosis in the chimpanzee brain.

2 | METHODS

2.1 | Specimens and sample processing

Postmortem formalin-fixed brain specimens from the dorsolateral prefrontal cortex (DLPFC, Brodmann areas 9/10) of 31 chimpanzees (*Pan troglodytes*) were provided by the National Chimpanzee Brain Resource (NCBR; NIH grant: NS092988; Table 1). Available medical history information is reported in Table 1 (Edler et al., 2017). Fixed chimpanzee brain samples were collected upon natural death or euthanasia due to medical concerns and immersion fixed in 10% formalin. After a minimum of 7 days, brains were transferred to a .1% sodium azide solution containing .1 M phosphate-buffered saline (PBS) and stored at 4°C. Samples were cryoprotected in a graded series of sucrose solutions before sectioning at a 40-μm thickness on a freeze sliding microtome (SM2000R, Leica, Chicago, IL). Each tissue section was placed in a single sequentially numbered centrifuge tube containing 30% dH_2O, 30% ethylene glycol, 30% glycerol, and 10% .244 M PBS and stored at −20°C until further histological or immunohistochemical processing. A 1:10 series was stained for Nissl substance using .5% cresyl violet to visualize cytoarchitecture and quantify total neuron and glia densities.

Layers I, III, and white matter (WM) of the DLPFC were analyzed in this study. This region was selected due to its role in both episodic and working memory tasks, which has shown increased vulnerability to aging in humans (Autrey et al., 2014; Bauer & Fuster, 1976; Brickman et al., 2007; Fuster & Alexander, 1971; Kane & Engle, 2002; Kubota & Niki, 1971; Miller & Orbach, 1972; Sherwood et al., 2011; Zimmerman et al., 2006). Layer I contains interlaminar astrocytes that are particularly susceptible to AD pathology in both humans and chimpanzees (Colombo et al., 2002, 2004; Munger et al., 2019). Layer III in the DLPFC shows increased astrogliosis and neuron loss in AD (Beach et al., 1989). The WM is also vulnerable to volumetric decline with age in both humans and nonhuman primates in the DLPFC as demonstrated by increased GFAP immunoreactivity (Allen et al., 2005; Autrey et al., 2014; Sherwood et al., 2011; Sloane et al., 2000).

2.2 | Antibody characterization

All primary antibodies are listed in Table 2. An equidistant series (~1:10) of brain sections containing the DLPFC was immunohistochemically processed for the following antibodies: (1) GFAP, a common marker for astrocytes; (2) excitatory amino acid transporter 2 (EAAT2), a glutamate transporter expressed predominantly in astrocytes; (3) glucose transporter 1 (GLUT1), a transporter in astrocytes; and (4) ionized calcium-binding adaptor molecule 1 (Iba1), a microglial marker. GFAP (Millipore, AB5804) is the main component of intermediate filaments in astrocytes, and specificity has been evaluated by immunohistochemistry in mouse, rat, and human brain tissue by the manufacturer. We also previously characterized GFAP using immunohistochemistry in chimpanzee brain samples (Munger et al., 2019). EEAT2 (Millipore, AB1783) removes L-glutamate, the primary excitatory neurotransmitter in the mammalian central nervous system (CNS), from the synaptic cleft, which helps maintain the proper diffusion gradient and prevent excitotoxicity. Specificity of the EEAT2 antibody was confirmed by Western blot using mouse brain membrane lysates by the manufacturer. The GLUT1 (Abcam, ab40084) isoform of glucose transporter is present in astrocytes surrounding blood vessels in the gray matter, and its specificity was evaluated by Western blot in HeLa cells and by immunohistochemistry in formalin-fixed human dermal carcinoma tissue sections by the manufacturer. Iba1 (Wako, 019-19741) is conserved in rat and human Iba1 protein sequences, and antibody specificity has been confirmed using immunohistochemistry in rodent, primate, and human brain samples (Imai et al., 1996). Additionally, sections from the DLPFC of six chimpanzees that exhibited widespread and severe astrogliosis were immunohistochemically processed and assessed for AD neuropathologic markers including amyloid precursor protein/Aβ (6E10, Biolegend, 803007) and phosphorylated tau (AT8, ThermoFisher, MN1020) as previously described (Edler et al., 2017). In AD, accumulation of aggregated Aβ peptides occurs in extracellular senile plaques and vasculature, while hyperphosphorylated tau forms pretangle and NFT in neurons, and both lesions are associated with glial activation (Montine et al., 2012; Serrano-Pozo et al., 2011). Antibody specificity for 6E10 and AT8 was confirmed by Western blot by the manufacturer and by immunohistochemistry in nonhuman primates (Edler et al., 2017; Goedert et al., 1995; Kim et al., 1988; Perez et al., 2013; Rosen et al., 2008).

2.3 | Immunohistochemistry

The avidin-biotin-peroxidase method was used for immunohistochemical processing of formalin-fixed chimpanzee brain samples. Briefly, tissue sections were pretreated for antigen retrieval (except EAAT2 sections) for 30 min in a .05% citraconic acid solution (pH 7.4) at 85°C. Endogenous peroxidase was quenched for 20 min using a solution of 75% methanol, 2.5% hydrogen peroxide (30%), and 22.5% dH_2O. Sections were blocked in PBS, Triton X-100, normal serum, and bovine serum albumin (BSA), except EAAT2 sections which were blocked in PBS, normal serum, BSA, and dried carnation milk. Sections were incubated in the primary antibodies GFAP, EEAT2, and GLUT1 (Table 2) for 24 h at room temperature (RT) followed by 24 h at 4°C, while sections processed for Iba1, 6E10, and AT8 primary antibodies were incubated at 4°C for 48 h. Sections were incubated in the appropriate biotinylated secondary antibody (1:200) and normal serum for 1 h at RT, before being placed in avidin-peroxidase

TABLE 1 Age (y), sex, astrogliosis classification, AD-related neuropathology, and available cause of death/notable medical history for chimpanzees used in stereological quantification

Age	Sex	Astrogliosis	Aβ	Tau	Stereology markers	Cause of death/notable medical history
12	F	Extreme	V	NC	GFAP, Iba1 EEAT2, GLUT1, Nissl	Peritonitis, focal pleuritis, callosities ulceration, inguinal/axillary lymphadenopathy
16	F	Moderate	n/a	n/a	GFAP, Iba1, Nissl	Trauma, thrombocytopenia, myocardial fibrosis
17	M	Severe	–	–	GFAP, Iba1, Nissl	Myocardial fibrosis
17	M	Extreme	–	NC	GFAP, Iba1 EEAT2, GLUT1, Nissl	n/a
19	F	Extreme	–	–	GFAP, Iba1 EEAT2, GLUT1, Nissl	n/a
19	M	Moderate	–	–	GFAP, Iba1, Nissl	Diabetes, meningitis, multifocal stomach hemorrhages, renal failure
19	M	Extreme	–	–	GFAP, Iba1 EEAT2, GLUT1, Nissl	Trauma
20	M	Extreme	–	–	GFAP, Iba1 EEAT2, GLUT1, Nissl	n/a
21	M	Severe	–	–	GFAP, Iba1, Nissl	n/a
21	F	Moderate	n/a	n/a	GFAP, Iba1, Nissl	Cardiomyopathy
24	M	Mild	n/a	n/a	GFAP, Iba1 EEAT2, GLUT1, Nissl	Myocardial fibrosis
27	F	Extreme	–	–	GFAP, Iba1 EEAT2, GLUT1, Nissl	n/a
35	F	Mild	–	–	GFAP, Iba1 EEAT2, GLUT1, Nissl	n/a
37	F	Severe	V	NC	GFAP, Iba1, Nissl	Peritonitis, necrotic bowel, uterine rupture
39	F	Moderate	V	–	GFAP, Iba1, Nissl	Heart failure
39	M	Moderate	V	NFT	GFAP, Iba1, Nissl	Heart failure, leprosy
40	F	Moderate	–	–	GFAP, Iba1, Nissl	Possible arrhythmia with trauma
40	F	Moderate	V	–	GFAP, Iba1 EEAT2, GLUT1, Nissl	n/a
40	M	Moderate	V	–	GFAP, Iba1 EEAT2, GLUT1, Nissl	Emaciation
41	M	Severe	V, P	NC	GFAP, Iba1, Nissl	Intestinal mass, HIV, hepatitis C
41	M	Moderate	V	NC	GFAP, Iba1 EEAT2, GLUT1, Nissl	n/a
41	F	Mild	V	–	GFAP, Iba1, Nissl	Chronic pleuritis, thoracic/lumbar spondylosis, degenerative joint disease, hemoperitoneum
43	F	Moderate	V, P	–	GFAP, Iba1 EEAT2, GLUT1, Nissl	Ischemic stroke
45	F	Mild	V, P	NFT, NC	GFAP, Iba1, Nissl	Heart failure, enlarged liver, respiratory failure
46	M	Moderate	V	–	GFAP, Iba1, Nissl	Chronic myocardial disease, endocarditis, hepatitis C, GERD
49	F	Moderate	V, P	NFT	GFAP, Iba1, Nissl	n/a
51	F	Mild	V, P	–	GFAP, Iba1, EEAT, GLUT1, Nissl	Heart failure

TABLE 1 (Continued)

Age	Sex	Astrogliosis	Aβ	Tau	Stereology markers	Cause of death/notable medical history
57	M	Moderate	V, P, Severe CAA	NFT, NC	GFAP, Iba1, Nissl	Congestive heart failure, colitis, arthritis
58	F	Moderate	V, P	NC	GFAP, Iba1, Nissl	Brain/aorta atherosclerosis
58	F	Mild	V, P, Severe CAA	NFT	GFAP, Iba1, Nissl	Breast cancer
62	M	Severe	V, P, Severe CAA	NFT	GFAP, Iba1, Nissl	Heart disease, hepatitis A and B

Note: Stereology variables were quantified for each chimpanzee based on tissue availability and are denoted as follows: (1) GFAP-ir and EEAT-ir astrocyte densities and soma volumes; (2) GLUT1-ir vessel volume; (3) Iba1-ir microglia density and morphologies; and (4) Nissl neuron and glia densities and glia:neuron ratio.

Abbreviations: M, male, F, female, V, vessels, P, plaques, CAA, cerebral amyloid angiopathy, NC, neuritic cluster, NFT, neurofibrillary tangle, n/a, not available.

TABLE 2 Primary antibodies used for immunohistochemical processing

Antigen	Immunogen	Dilution	Company, catalog #	RRID
GFAP	Rabbit polyclonal to purified bovine glial fibrillary acidic protein	1:12,500	Millipore, AB5804	AB_2109645
EAAT2	Guinea pig polyclonal to synthetic peptide from the carboxy-terminus of rat GLT-1	1:3000	Millipore, AB1783	AB_90949
GLUT1	Mouse monoclonal to glucose transporter 1	1:5000	Abcam, ab40084	AB_2190927
Iba1	Rabbit polyclonal to C-terminus of amino acids 81–93 of human AIF-1	1:10,000	Wako, 019-19741	AB_839504
APP/Aβ (6E10)	Mouse monoclonal to amino acid residue 1–16 of beta amyloid (DAEFRHDSGYEVHHQK)	1:7,500	Biolegend, 803007 (formerly Covance, SIG-39320)	AB_2564657
Tau (AT8)	Mouse monoclonal to paired helical filaments-tau phosphoSer202 and phosphoThr205	1:2500	ThermoFisher, MN1020	AB_223647

complex (PK-6100, Vector Laboratories, Burlingame, CA, USA) followed by 3, 3′-diaminobenzidine-peroxidase substrate with nickel enhancement (SK-4100, Vector Laboratories) or NovaRED (SK-4800, Vector Laboratories) for visualization. Sections were mounted on slides, dehydrated in an ethanol series, and coverslipped using DPX.

2.4 | Characterization of astrogliosis, microglial activation, and AD pathology

Astrogliosis is a graded response that occurs in concordance with the severity and progression of the underlying condition from mild to severe (Figure 1) (Heneka et al., 2010; Sofroniew, 2009; Sofroniew & Vinters, 2010). Astrocyte phenotype in healthy CNS tissue includes low levels of GFAP, nonoverlapping domains, and a lack of cellular proliferation. Mild astrogliosis is defined by a small, dispersed upregulation of GFAP, some hypertrophy of the cell soma, and little to no astrocyte proliferation, although domain organization remains intact and interlaminar astrocytes are unaffected (Figure 1a,e). Moderate astrogliosis includes an increase in GFAP expression in the upper cortical layers (i.e., layers I-IV) with marked hypertrophy of the soma and processes but limited proliferation. Clustering of astrocytes near areas of trauma, infection, or pathology and disruption of the interlaminar palisade are observed at this stage (Figure 1b,f). Lastly, severe astrogliosis is defined by dramatic upregulation of GFAP through all cortical layers, significant hypertrophy of cell soma and processes, proliferation, and a loss of domain organization. Furthermore, the interlaminar astrocyte palisade breaks down and decreased astrocyte density in cortical layer I can occur (Figure 1c,g) (Colombo et al., 2002, 2004; Munger et al., 2019).

To evaluate if astrogliosis levels correlated with microglial activation, we utilized total microglia and morphological subtype (ramified, intermediate, and amoeboid) densities collected in 18 chimpanzees from a prior study and quantified 13 additional chimpanzees as previously described (Figure 1i–k) (Edler et al., 2018; Kettenmann et al., 2011). Briefly, resting microglia have a ramified morphology with a small cell soma and long, highly arborized processes that survey the cellular environment (Streit et al., 1999). In the presence of pathology, infection, or trauma, microglia activate, which can be

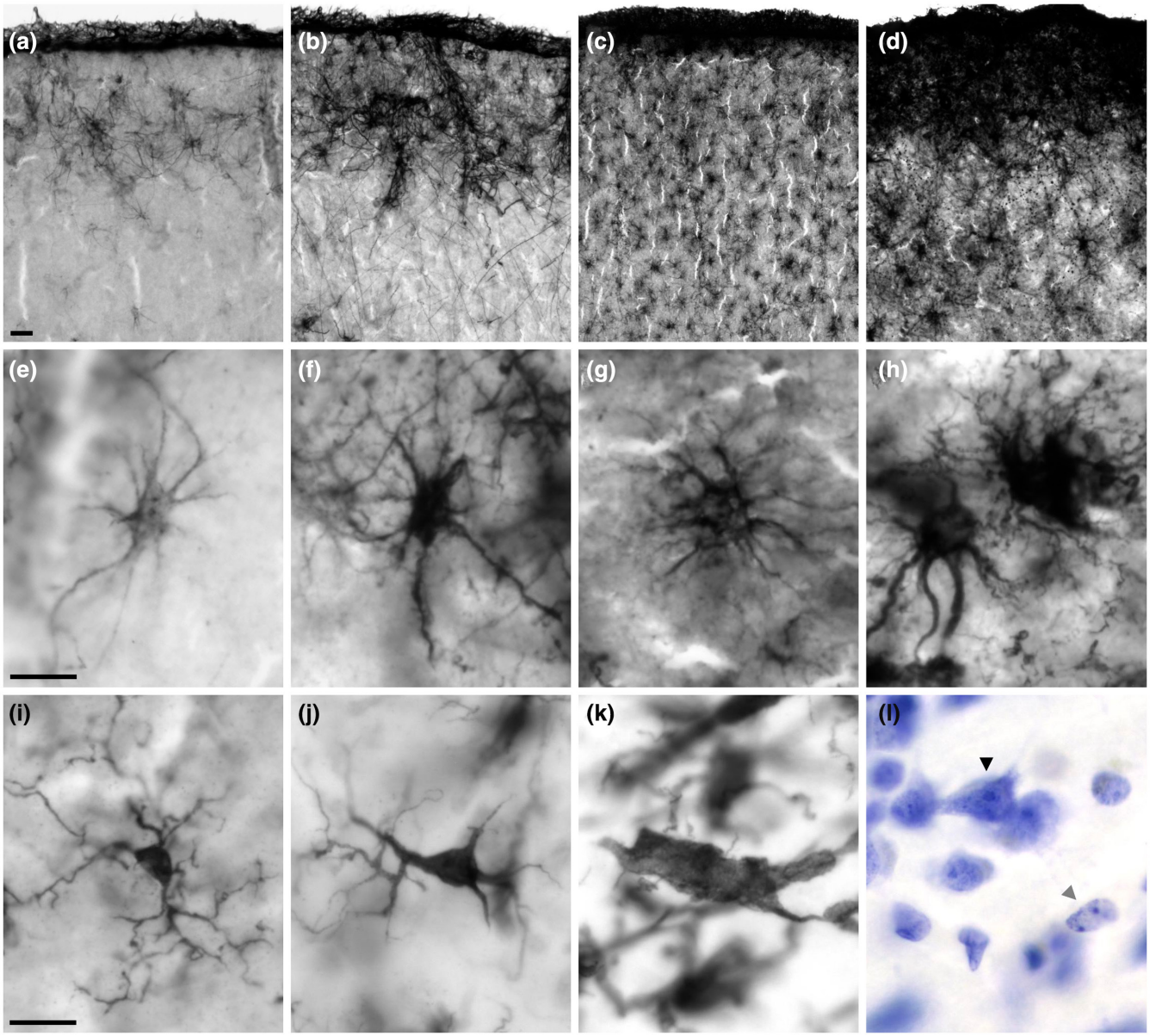

FIGURE 1 Photomicrographs of astrogliosis levels (a–h), microglia morphologies (i–k), and Nissl-positive neurons (black arrow) and glia (gray arrow, l) in DLPFC layer I of chimpanzees. Astrogliosis levels included healthy/mild (a, e), moderate (b, f), severe (c, g), and extreme (d, h). Chimpanzees with extreme astrogliosis displayed extensive upregulation of GFAP across cortical layers and in the WM with definite hypertrophy and complete loss of domain organization. Microglia use highly motile ramified processes to survey the cellular environment in their resting state (i), but upon activation, they exhibit a phenotypic graded response of decreased arborization, enlarged cell soma, and shortened (intermediate, j) or total loss of cellular processes (amoeboid, k). DLPFC, dorsolateral prefrontal cortex, GFAP, glial fibrillary acidic protein, WM, white matter. Scale bars: 25 μm.

visualized as two distinct morphological subtypes, intermediate and amoeboid (Kettenmann et al., 2011). Intermediate microglia have enlarged cell somas with shorter, thicker, and less arborized processes compared to ramified microglia, while amoeboid microglia are involved in the process of phagocytosis and marked by an enlarged, irregular-shaped cell soma and an absence of processes.

Our team previously evaluated DLPFC brain samples from 20 aged apes, along with eight younger chimpanzees in the current study, for AD-like pathology including Aβ-ir plaques, Aβ-ir vessels, cerebral amyloid angiopathy (CAA, amyloid deposition in the brain's vasculature), NFT, and tau neuritic clusters (NC, aggregates of tau-positive dystrophic neurites which are unique to chimpanzees; Table 1) (Edler et al., 2017). Tau and Aβ lesions were categorized as outlined in Serrano-Pozo et al. (2011), although Aβ-ir diffuse and dense-core plaques were not quantified separately in chimpanzees (Serrano-Pozo et al., 2011).

2.5 | Stereology

Quantitative analyses were performed using computer-assisted stereology with an Olympus BX-51 photomicroscope equipped

TABLE 3 Stereology sampling parameters

Antigen	Stereology variables	DLPFC layer	*n*	Probe	Counting frame (μm)	Disector height (μm)	Avg sec thickness (μm)	Avg sampling sites	Avg CE
GFAP	Av + SV	Lay I	31	Optical fractionator with nucleator	100 × 100	7–10	11.56	135 ± 16	.09
		Lay III					12.17	133 ± 15	.08
		WM					13.33	127 ± 10	.12
EEAT2	Av + SV	WM	13	Optical fractionator with nucleator	50 × 50	8	10.50	75 ± 8	.08
Iba1	Total Mv, Ramified Mv, Intermediate Mv, Amoeboid Mv	Lay III	31	Optical fractionator	250 × 250	8	14.01	45 ± 11	.07
Nissl	Total Nv, Total Gv	Lay I	13	Optical fractionator	75 × 75	10	11.98	70 ± 8	Nv = .19, Gv = .05
		Lay III					13.63	68 ± 7	Nv = .05, Gv = .05
		WM					16.03	72 ± 8	Nv = .24, Gv = .04
GLUT1	Vessel volume	Lay I-VI	13	Area fraction fractionator	300 × 300 (point grid)	–	–	63 ± 6	.03

with StereoInvestigator software (Version 11, MBF Bioscience, Williston, VT). Initial subsampling techniques were conducted for each probe to determine appropriate sampling parameters (Slomianka & West, 2005). Stereological evaluation was performed blinded to age and sex for astrocyte densities (Av, mm^3) and soma volumes (SV, μm^3) for GFAP and EEAT2, volume occupied by GLUT1-ir vessels (% area fraction, AF), Iba1-ir microglia (Mv, mm^3) and morphology densities (ramified Mv, intermediate Mv, amoeboid Mv, mm^3), and total neuron (Nv, mm^3) and glia (Gv, mm^3) densities (Nissl). Stereological parameters, including region of interest (i.e., layers of DLPFC), number of individuals (n), probe, counting frame, disector height, and average CE for each variable, are reported in Table 3. Briefly, for all cell densities, the optical fractionator probe was used at 40× (.75 N.A., GFAP, Iba1) or 60× (1.42 N.A., EEAT2, Nissl) with a 2% guard zone and section thickness measured every fifth sampling site. All cells of interest within the counting frame were counted. For GFAP and EEAT2, SVs were measured for every second or third marked astrocyte simultaneously using the nucleator probe, and six rays were used to define the soma edges. Cell densities were calculated as the layer-specific estimated population divided by the planimetric volume of the region of interest. The volume of GLUT1-ir vessels was quantified at 10× (.25 N.A.) with the area fraction fractionator probe (AFF), which uses a Cavalieri point counting system. Every point on the grid received one of two markers: non-GLUT1-ir vessel or GLUT1-ir vessel. Estimated AF was calculated as a percentage of the tissue occupied by GLUT1-ir vessels across all layers of the DLPFC.

2.6 | Statistical analyses

Data were examined for outliers, which SPPS considers if they extend more than 1.5 box-lengths from the edge of the box, and outliers were removed prior to analyses. Two-way mixed-effects ANOVAs were utilized to investigate subregional differences (within-subjects factors: layers I and III, WM) in Av and SV between astrogliosis levels, and Bonferroni post-hoc tests were performed. One-way ANOVAs or Kruskal–Wallis tests were used to identify variation in Mv and morphologies (ramified, intermediate, amoeboid), Nissl (Nv, Gv, G:N ratio), EEAT2 (Av, SV), and GLUT1 (% volume) data with a Bonferroni correction. The association of the presence of AD pathologies (i.e., Aβ: plaques and vessels; tau: NFT and NC) with cell densities (Av, Sv, Mv, Nv, Gv) and G:N ratio were examined with independent samples *t*-tests or one-way ANOVAs. When the Levene's statistic was significant, the t value for equal variances not assumed and the Brown–Forsythe *F* and *p* values were reported. Age-related differences in GFAP-ir Av and SV, Iba1-ir Mv and morphologic densities, and Nissl Nv, Gv, and G:N ratios were analyzed using simple linear regression. Unpaired *t*-tests (Av, SV) or Mann–Whitney tests (Mv) were utilized to determine the association of sex. All statistical analyses were performed using IBM SPSS (Version 28) and Statistica (Version 13), and alpha was set at .05.

3 | RESULTS

3.1 | Effect of astrogliosis level on cell density and ratio

The degree of astrogliosis ranged from healthy to severe in the DLPFC of chimpanzees. In addition, six chimpanzees exhibited "extreme" astrogliosis indicative of potentially global CNS inflammation that scaled beyond the other chimpanzees in the study (Table 1; Figure 1d,h). Like chimpanzees with severe astrogliosis, the astrocytes in chimpanzees with extreme astrogliosis displayed extensive upregulation of GFAP across cortical layers and in the WM with definite hypertrophy and complete loss of domain organization. The interlaminar palisade was lost, although hypertrophic layer I astrocytes remained. Some astrocytes had a granular/fuzzy phenotype (GFA) with fine dotted branching processes and a tau-ir soma, and astrogliosis was routinely observed in association with vasculature in these animals (Figure 2b).

Chimpanzees with extreme astrogliosis displayed minimal AD-like pathology with the occasional presence of an AT8-ir pretangle and tau neuritic cluster (NC) in layers III and V in two apes and an Aβ-ir vessel in the WM of one ape. NFT and Aβ-ir plaques were

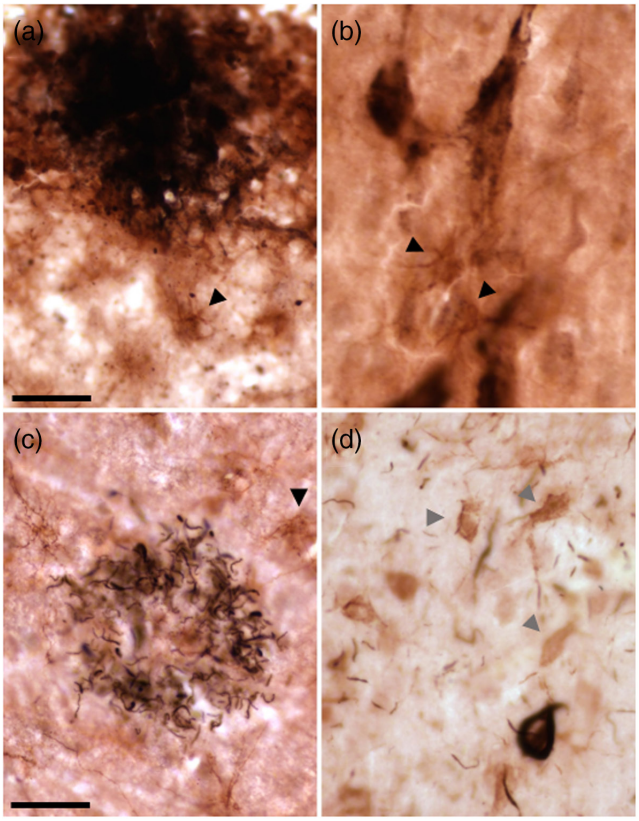

FIGURE 2 Photomicrographs of GFAP-ir astrocytes (black arrows, a–c) and Iba1-ir microglia (gray arrows, d) in chimpanzees with a Aβ-ir dense-core plaque (a), Aβ-ir vessels (b), a tau NC (c), and a NFT (d). GFAP, glial fibrillary acidic protein, Iba1, ionized calcium-binding adaptor 1, Aβ, amyloid-beta, NC, neuritic cluster, NFT, neurofibrillary tangle. Scale bar: 25 μm.

completely absent, although Aβ was observed in a diffuse, punctuate pattern in the cell soma of layer III–VI neurons. Surprisingly, tau-ir astrocytes were not observed in the "extreme" astrogliosis chimpanzees. In a few chimpanzees, tau deposition appeared in a linear, bead-like fashion in layers I–IV and seemed located in varicosities of interlaminar astrocytes. However, additional immunolabeling is needed to determine cellular localization.

To determine if chimpanzees with extreme astrogliosis exhibited changes in Av and SV compared to chimpanzees in the well-established categories of healthy/mild, moderate, and severe astrogliosis, we compared GFAP-ir Av and SV in layers I, III, and WM in the DLPFC of 31 chimpanzees (Table 4; Figure 3a,b). A two-way mixed-effects ANOVA found significant main effects for region ($F_{2,54} = 19.64$, $p < .01$) and astrogliosis level ($F_{3,27} = 7.15$, $p = .01$) with a nonsignificant interaction ($F_{6,54} = .93$, $p = .48$) in GFAP-ir Av. Bonferroni post-hoc testing determined that chimpanzees with extreme astrogliosis had greater GFAP-ir Av compared to all other astrogliosis levels in layer I (p's $< .03$), and that Av was higher in layer I than layer III and WM (p's $< .01$; Figure 3a). GFAP-ir SV showed a significant main effect for region ($F_{2,54} = 38.84$, $p < .01$) and nonsignificant main effect for astrogliosis level ($F_{3,27} = 1.58$, $p = .22$) and interaction ($F_{6,54} = .68$, $p = .67$; Figure 3b). Bonferroni post-hoc tests revealed that GFAP-ir SV in the WM, regardless of astrogliosis level, was lower than layers I and III (p's $< .04$; Figure 3b). In addition, EAAT2-ir WM Av, EAAT2-ir WM SV, and % of volume occupied by GLUT1-ir vessels in gray matter of the DLPFC were collected in 13 chimpanzees categorized as having mild, moderate, or extreme astrogliosis. Using independent samples Kruskal–Wallis tests with a Bonferroni adjustment ($n = 2$ tests, $\alpha = .03$), we found that average EAAT2-ir Av, and EAAT2-ir SV did not change based on astrogliosis level (p's $> .05$; data not shown). One-way ANOVA also determined no significant difference in % of volume occupied by GLUT1-ir vessels by astrogliosis level ($F_{2,10} = 3.10$, $p = .09$; data not shown).

Iba-ir Mv and morphological densities were compared in layer III of the DLPFC by astrogliosis level (Table 4). One-way ANOVA determined that total Mv ($F_{3,27} = 1.16$, $p = .34$), ramified Mv ($F_{3,23} = .53$, $p = .67$), and intermediate Mv ($F_{3,25} = .77$, $p = .52$) were not associated with astrogliosis level (Figure 3c). The Levene's statistic for homogeneity of variance was significant for amoeboid Mv ($p = .32$). Therefore, a Kruskal–Wallis test was performed, and amoeboid Mv was not correlated with astrogliosis level ($H_{29} = 6.07$, $p = .11$).

Nissl Nv, Gv, and G:N ratio were measured in layer III of the DLPFC (Table 4). One-way ANOVA was nonsignificant for Nissl Nv ($F_{3,27} = 1.06$, $p = .38$), Gv ($F_{3,27} = 1.19$, $p = .33$), and G:N ratio ($F_{3,27} = .96$, $p = .43$) based on astrogliosis levels (Figure 3d–f).

3.2 | Effect of AD-like pathology on cell density and ratio

Chimpanzees with significant Aβ and tau lesions displayed astrogliosis primarily in proximity to pathologic lesions and near blood vessels and appeared to have fewer layer I GFAP-ir astrocytes and a loss of the interlaminar palisade (Figure 2a–c). Yet, severe hypertrophic phenotypes in reactive astrocytes and widespread upregulation of GFAP were absent. These observations differed from chimpanzees with extreme astrogliosis, which demonstrated widespread GFAP upregulation, hypertrophy, cell clustering throughout the cortical layers, overlapping processes of interlaminar astrocytes, and minimal AD pathology (Figure 1d,h).

To examine if specific types of AD pathology were associated with changes in astrocyte, microglia, neuron, and glia densities in the DLPFC, we used immunohistochemical data collected in a prior investigation and in the current study to categorize 28 chimpanzees based on the presence of five types of AD pathology: (1) Aβ-ir plaques, (2) Aβ-ir vessels (mild to moderate CAA), (3) severe CAA, (4) NFT, and (5) tau NC (Table 1) (Edler et al., 2017). Cell densities/ratio in apes with Aβ or CAA were compared to those without Aβ lesions, while chimpanzees with NFT and tau NC were compared to individuals lacking tau lesions using independent samples t-tests (Bonferroni corrected $\alpha = .02$ for Av/SV/Nv/Gv/G:N or $\alpha = .01$ for Mv) or one-way ANOVAs with Bonferroni post-hoc ($\alpha = .05$; Tables 4–6). For Av, SV, Nv, Gv, and G:N ratio, independent samples t-tests found no significant differences regardless of layer in chimpanzees with Aβ-ir plaques versus those without (Table 5; Figure 4a,b). In contrast, ramified Mv was lower in chimpanzees with Aβ-ir plaques and NFT (p's $\leq .01$; Figure 4d), while chimpanzees with Aβ-ir vessels had significantly reduced total and ramified Mv yet greater amoeboid Mv (p's $< .01$; Figure 4c–e). Apes with Aβ-ir vessels, but not CAA, had reduced Av in layer I and WM (p's $\leq .01$; Figure 4a,b) compared to those without Aβ pathology, although apes with severe CAA had lower ramified Mv ($p = .04$; Figure 4d). Nv, Gv, and G:N ratio did not vary based on the presence or absence of Aβ-ir vessels or severe CAA (p's $\geq .58$). Neither tau lesion (i.e., NFT or NC) was associated with changes in Av or Sv in any layer (p's $\geq .36$; Table 5). However, ramified Mv was significantly lower in apes with NFT ($p = .002$; Figure 4c), although no differences were observed in Mv with tau NC (p's $\geq .11$). NFT lesions did not affect Nv, Gv, or G:N ratio (p's $\geq .10$). Additionally, we omitted chimpanzees with extreme astrogliosis and performed the same analyses (Table 6). AD pathology did not affect Av, SV, Nv, or G:N ratio. However, one-way ANOVA with a Bonferroni post-hoc test determined that chimpanzees with Aβ-ir vessels or severe CAA had fewer ramified Mv compared to those without Aβ lesions (p's $\leq .02$; Figure 4f), while chimpanzees with tau NC had higher Gv than animals lacking tau lesions ($p = .02$; Figure 4g).

3.3 | Association of age and sex on cell density and ratio

GFAP-ir Av was quantified in layer I, layer III, and WM, while Mv, Nv, Gv, and G:N ratios were collected in layer III of the DLPFC. Simple linear regression analyses revealed no association of age on GFAP-ir Av or SV in layer I (Av: $R^2 = .00$, $p = .88$; SV: $R^2 = .00$, $p = .92$), layer III (Av: $R^2 = .09$, $p = .10$; SV: $R^2 = .01$, $p = .68$), or WM (Av: $R^2 = .03$,

TABLE 4 Average cell densities (mm^3) and standard deviations for astrocytes (Av), microglia (Mv), neurons (Nv), and glia (Gv), soma volumes (SV) for astrocytes, and glia: neuron ratios (G:N) in the DLPFC of chimpanzees by astrogliosis level or type of AD lesion

	Astrogliosis level				
	Subregion/Morphology	**Mild**	**Moderate**	**Severe**	**Extreme**
GFAP-ir Av	Layer I	3688 ± 1938	3871 ± 1503	3421 ± 2324	8529 ± 5891
	Layer III	1081 ± 209	1609 ± 930	2490 ± 935	5357 ± 4488
	WM	1240 ± 693	1609 ± 531	1882 ± 594	4034 ± 2998
GFAP-ir SV	Layer I	356 ± 117	507 ± 252	414 ± 142	471 ± 99
	Layer III	316 ± 59	456 ± 192	392 ± 145	408 ± 106
	WM	137 ± 23	184 ± 75	152 ± 47	255 ± 43
Iba1-ir Mv (Layer III)	Total	6062 ± 2094	6859 ± 3684	6393 ± 2440	9379 ± 5476
	Ramified	2075 ± 2400	1522 ± 2709	2662 ± 2599	2960 ± 1782
	Intermediate	2756 ± 2549	4773 ± 4281	3501 ± 2217	6356 ± 6860
	Amoeboid	239 ± 250	419 ± 409	136 ± 142	62 ± 55
Nissl (Layer III)	Nv	34,484 ± 6195	37,369 ± 9519	30,882 ± 8475	38,842 ± 6375
	Gv	58,258 ± 10,326	54,614 ± 17,743	50,631 ± 18,577	67,419 ± 15,128
	G:N	1.71 ± .30	1.48 ± .40	1.62 ± .39	1.76 ± .45
	AD pathology				
	Subregion/Morphology	**Aβ negative**	**Aβ plaque**	**Aβ vessel**	**CAA**
GFAP-ir Av	Layer I	7207 ± 4868	4022 ± 1789	3188 ± 961	5289 ± 2578
	Layer III	3811 ± 3978	1687 ± 918	1665 ± 769	1945 ± 940
	WM	3116 ± 2587	1408 ± 573	1334 ± 503	1585 ± 750
GFAP-ir SV	Layer I	444 ± 114	486 ± 215	517 ± 243	327 ± 89
	Layer III	410 ± 123	428 ± 169	451 ± 185	298 ± 23
	WM	212 ± 70	185 ± 94	160 ± 30	242 ± 162
Iba1-ir Mv (Layer III)	Total	9797 ± 4855	5852 ± 2293	5743 ± 2084	6867 ± 173
	Ramified	2932 ± 1887	452 ± 371	818 ± 1579	504 ± 562
	Intermediate	6271 ± 6468	4457 ± 1562	4093 ± 1836	5739 ± 299
	Amoeboid	80 ± 87	396 ± 305	585 ± 606	442 ± 97
Nissl (Layer III)	Nv	36,748 ± 8284	34,495 ± 9218	35,894 ± 8864	31,946 ± 4142
	Gv	59,193 ± 17,049	55,169 ± 13,174	56,234 ± 18,272	47,217 ± 10,168
	G:N	1.60 ± .24	1.62 ± .22	1.60 ± .49	1.47 ± .13
	AD pathology				
	Subregion/Morphology	**Tau negative**	**NFT**	**NC**	
GFAP-ir Av	Layer I	5577 ± 4242	4462 ± 1934	3898 ± 2473	
	Layer III	2669 ± 3265	1736 ± 768	2342 ± 1518	
	WM	2296 ± 2154	1396 ± 578	1561 ± 1242	
GFAP-ir SV	Layer I	485 ± 203	465 ± 269	438 ± 106	
	Layer III	431 ± 162	408 ± 196	390 ± 117	
	WM	186 ± 51	195 ± 118	203 ± 113	
Iba1-ir Mv (Layer III)	Total	8162 ± 4435	6635 ± 2308	5522 ± 2005	
	Ramified	2090 ± 2048	377 ± 449	1302 ± 1949	
	Intermediate	5743 ± 5290	4835 ± 1397	3917 ± 2231	
	Amoeboid	331 ± 555	542 ± 407	335 ± 348	
Nissl (Layer III)	Nv	36,047 ± 8613	30,923 ± 3020	38,041 ± 8582	
	Gv	53,095 ± 19,013	51,555 ± 8331	67,030 ± 11,037	
	G:N	1.47 ± .36	1.67 ± .26	1.82 ± .43	

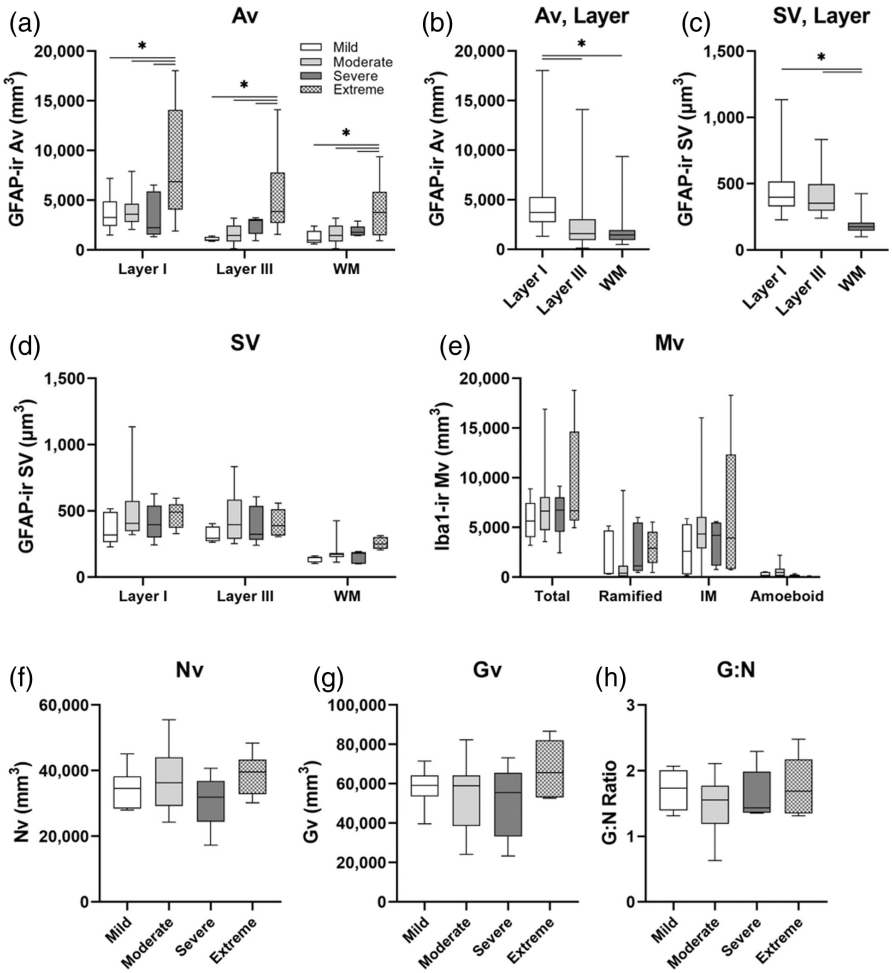

FIGURE 3 Boxplots of GFAP-ir Av (a, b) and SV (c, d), Iba1-ir Mv (e), and Nissl Nv (f), Gv (g), and G:N ratio (h) by astrogliosis levels. Chimpanzees with extreme astrogliosis had significantly greater Av compared to all other levels in layer I (a). Av was greatest in layer I (b), while SV was reduced in the WM (c). In contrast, astrogliosis levels were not associated with changes in SV (d), Mv (e), Nv (f), Gv (g), or G:N ratio (h). GFAP, glial fibrillary acidic protein, Av, astrocyte density, SV, astrocyte soma volume, Iba1, ionized calcium-binding adaptor 1, Mv, microglia density, Nv, neuron density, Gv, glia density, G:N, glia to neuron, WM, white matter.

$p = .41$; SV: $R^2 = .12$, $p = .06$). Age also was not correlated with changes in Nissl Nv ($R^2 = .05$, $p = .22$), Gv ($R^2 = .00$, $p = .95$), G:N ratio ($R^2 = .06$, $p = .17$), Iba1-ir total Mv ($R^2 = .02$, $p = .48$), or intermediate Mv ($R^2 = .03$, $p = .36$) in layer III of the DLPFC. In contrast, Iba1-ir ramified Mv significantly decreased with age ($R^2 = .44$, $p < .01$), while amoeboid Mv increased with age ($R^2 = .50$, $p < .00$; Figure 5). Sex had no association with GFAP-ir Av and SV (all p's $> .04$, multiple comparison testing bias adjusted $\alpha = .01$), Nissl Nv, Gv, and G:N ratios (all p's $> .06$; adjusted $\alpha = .02$), or Iba1-ir Mv (all p's $> .38$; adjusted $\alpha = .01$) as determined by Mann–Whitney tests (GFAP: Av, SV; Iba1: Mv) for non-normal distribution of residuals and unpaired t-tests (Nissl: Nv, Gv, G:N) for normal distribution of residuals.

4 | DISCUSSION

Ranging from mild to severe, astrogliosis is a graded response to infection, neurodegeneration, or injury resulting in GFAP upregulation, soma hypertrophy, elongation of dendritic processes, and loss of domain organization (Heneka et al., 2010; Sofroniew & Vinters, 2010). Here, we report an extreme form of astrogliosis in the DLPFC of chimpanzees. In addition, chimpanzees with Aβ-ir vessels exhibited decreased Av, total Mv, and ramified Mv compared to those lacking pathology, while chimpanzees with tau NC had greater overall Gv and G:N ratios. Aging was associated with lower ramified Mv and higher amoeboid Mv but no changes in Av.

Extreme astrogliosis in the chimpanzee brain was characterized by extensive GFAP upregulation, increased Av in cortical layer I, and loss of domain organization and the interlaminar palisade in the absence of significant microglial activation and AD lesions (Figures 1 and 3). Chimpanzees with extreme astrogliosis were relatively young, ranging from 12 to 27 years old, compared to those with significant AD pathology (i.e., NFT or severe CAA), which were 39 to 62 years old, suggesting that age may be a factor. The average lifespan for chimpanzees is approximately 35 years (Che-Castaldo et al., 2021; Wood et al., 2017). Thus, the captive chimpanzees that died at a young age with extreme astrogliosis are not normative, as without significant disease or trauma, they typically would live

TABLE 5 Independent samples *t*-test and one-way ANOVA statistics for all chimpanzees with mild to extreme astrogliosis and with and without Aβ-ir plaques, Aβ-ir vessels, severe CAA, NFT, and tau NC

		Aβ plaques			Aβ vessels, CAA		
	Subregion/Morphology	*t*	*df*	*p*	*F*	*df*	*p*
GFAP-ir Av	Layer I	.85	26	.41	4.52	2, 11	.04**
	Layer III	1.09	26	.28	2.54	2, 11	.13
	WM	1.22	26	.23	3.99	2, 11	.05**
GFAP-ir SV	Layer I	−.28	26	.78	1.32	2, 25	.29
	Layer III	−.19	26	.85	2.32	2, 24	.12
	WM	.12	26	.90	.98	2, 3	.48
Iba1-ir Mv (Layer III)	Total	1.46	26	.16	5.77	2, 11	.02**
	Ramified	3.23	18	.01*	5.10	2, 21	.02**
	Intermediate	.48	24	.64	1.02	2, 10	.39
	Amoeboid	−.14	24	.89	7.40	2, 14	.01**
Nissl (Layer III)	Nv	.56	26	.58	.38	2, 25	.69
	Gv	.24	26	.81	.55	2, 25	.58
	G:N	−.32	26	.75	.10	2, 25	.87
		NFT			TAU NC		
	Subregion/Morphology	*t*	*df*	*p*	*t*	*df*	*p*
GFAP-ir Av	Layer I	.30	26	.77	.90	26	.38
	Layer III	.77	26	.45	.15	26	.88
	WM	.94	26	.36	.82	26	.42
GFAP-ir SV	Layer I	.08	26	.94	.55	26	.59
	Layer III	.21	26	.83	.64	26	.53
	WM	−.28	26	.78	−.52	26	.62
Iba1-ir Mv (Layer III)	Total	.50	26	.62	1.67	26	.11
	Ramified	3.19	22	.00*	.57	22	.57
	Intermediate	.17	24	.87	.97	24	.34
	Amoeboid	−.85	24	.40	.27	24	.79
Nissl (Layer III)	Nv	1.70	26	.10	−.93	26	.36
	Gv	.77	26	.45	−2.26	26	.03
	G:N	−.62	26	.54	−2.18	26	.04

Abbreviations: Aβ, amyloid-beta; CAA, cerebral amyloid angiopathy; NC, neuritic cluster; NFT, neurofibrillary tangle.

*denotes significance with a Bonferroni correction for multiple comparison testing with $\alpha \leq .02$ for Av, SV, Nv, Gv, G:N, and $\alpha \leq .01$ for Mv for t-tests; **denotes significance with a Bonferroni correction with $\alpha = .05$ for one-way ANOVA tests.

longer. Aging also can cause a gradual loss of function in astrocytes and microglia, dampening the response of these senescent cells to injury, infection, or neurodegeneration. High levels of astrogliosis in younger chimpanzees may occur, because these cells retain their full functional capabilities and can mount a strong neuroinflammatory response to what caused their death. Unfortunately, medical history was available for only two chimpanzees with extreme astrogliosis, including a 12-year-old female with peritonitis (Table 1). Peritonitis is inflammation of the inner lining of the abdominal wall, and it often is associated with infection from a perforated bowel or a ruptured appendix. Therefore, we postulate that extreme astrogliosis in the chimpanzee brain may be the result of systemic or peripheral inflammation due to pathogen or trauma. Prior evidence indicates that peripheral inflammation caused by infection or trauma can trigger a rapid and widespread cytokine release, inducing glial activation and leading to cognitive decline (Chen et al., 2008; Demers et al., 2018; Henry et al., 2009; Iwashyna et al., 2010; Perry et al., 2004; Terrando et al., 2010). For example, in cats with feline infectious peritonitis (FIP), cytokines IL-6, macrophage inhibitory protein-1 alpha, and RANTES are upregulated (Foley et al., 2003). Moreover, a recent study investigating CNS lesions in FIP found an increase in the number of protoplasmic astrocytes in the cerebrum, particularly in periventricular areas, with degenerative and necrotic lesions (Mesquita et al., 2016). Reactive astrocytes in these animals also had shorter processes, greater numbers of intermediate filaments, and increased GFAP immunoreactivity, but only a mild microglial

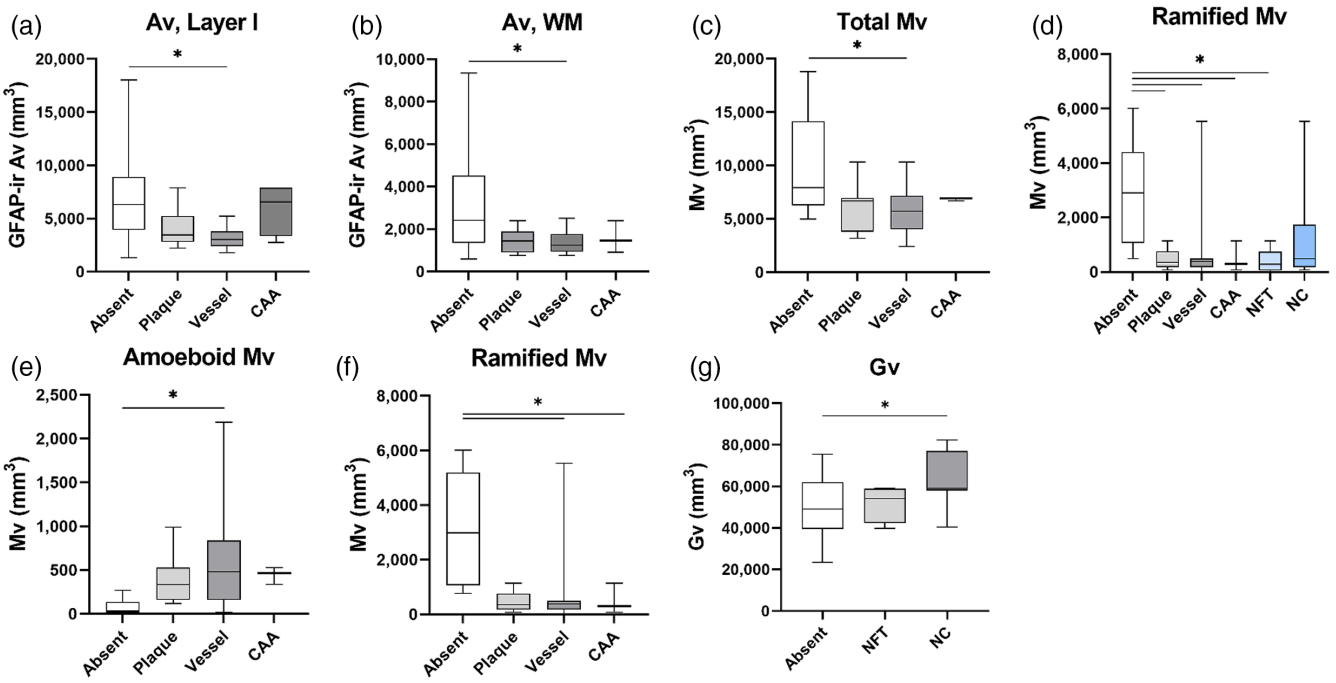

FIGURE 4 Boxplots of GFAP-ir Av (a, b), Iba1-ir Mv (c–f), and Nissl Gv (f) based on the absence or presence of Aβ (a–f: plaques, vessels, CAA) or tau lesions (d, g: NFT, NC) in all 31 chimpanzees. In layer I (a) and WM (b) of the DLPFC, Av was significantly lower in chimpanzees with Aβ-ir vessels compared to those without pathology. Total Mv also was reduced in chimpanzees with Aβ-ir vessels (c). Ramified Mv was significantly lower with all pathology types except tau NC (d), while amoeboid Mv was greater in chimpanzees with Aβ-ir vessels (e). In analyses omitting the six chimpanzees with extreme astrogliosis, ramified Mv was lower in apes with Aβ-ir vessels and CAA (f), while Gv was greater in chimpanzees with tau NC compared to those without these lesions (g). GFAP, glial fibrillary acidic protein, Av, astrocyte density, Iba1, ionized calcium-binding adaptor 1, Mv, microglia density, Gv, glia density, G:N, glia to neuron, Aβ, amyloid-beta, NC, neuritic cluster, NFT, neurofibrillary tangle, WM, white matter.

response despite severe lesions. Severe infections, such as peritonitis, are also commonly associated with sepsis, a blood infection that triggers systemic inflammation. In a study of patients who died from sepsis, pro-inflammatory microglial activation occurred primarily in the white matter with very little activation in the gray matter (Zrzavy et al., 2019). As we quantified Mv in layer III of the gray matter (DLPFC), this may explain the presence of extreme astrogliosis in layer I in the absence of microglial activation in the chimpanzee brain. Thus, further investigation of Mv in the white matter of chimpanzees with extreme astrogliosis is required.

Astrocytes and microglia are important players in the regulation of the inflammatory response to aging (Kettenmann et al., 2011; Sofroniew & Vinters, 2010). Increased oxidative stress with age leads to nuclear and cellular damage and increased pro-inflammatory cytokines which cause constant low-grade inflammation that triggers glial activation (Cotrina & Nedergaard, 2002; Dall'Olio et al., 2013; Finch, 2003; Franceschi, Bonafè, et al., 2000; Franceschi, Valensin, et al., 2000; Harman, 1956; Moller et al., 2010; Nichols et al., 1993; Poon et al., 2004; Rodier & Campisi, 2011). Consistent with our previous reports, physiological aging was not associated with changes in GFAP-ir Av and SV or Nissl Nv, Gv, or G:N ratio in the DLPFC of chimpanzees (Beach et al., 1989; Cotrina & Nedergaard, 2002; Edler et al., 2020; Munger et al., 2019; Nichols et al., 1993; Pelvig et al., 2008). Similarly, studies of rhesus macaques also did not find an increase in astrogliosis with age as measured by GFAP-ir Av, although aged astrocytes did have greater numbers of filaments in their processes (Haley et al., 2010; Kanaan et al., 2010; Peters et al., 2008, 2010; Robillard et al., 2016; Sloane et al., 2000). However, our results diverge from prior reports in humans and rodents that demonstrated an increase in GFAP mRNA, protein, and qualitative measures with age (Beach et al., 1989; David et al., 1997; Finch et al., 2002; Goss et al., 1991; Janota et al., 2015; Landfield et al., 1977; Morgan et al., 1997; Nichols et al., 1993; O'Callaghan & Miller, 1991). Elderly humans exhibited mild astrogliosis and GFAP upregulation in the WM, although like chimpanzees, overall astrocyte density did not vary with age (Beach et al., 1989; Cotrina & Nedergaard, 2002; Nichols et al., 1993; Pelvig et al., 2008). Some reports in rhesus macaques also identified significant increases with age when using methods examining volumetric change of overall GFAP expression (Cargill et al., 2012; Haley et al., 2010; Sloane et al., 2000). Thus, normal aging in the nonhuman primate CNS likely includes a shift of astrocyte phenotype, noted by hypertrophy of processes and loss of domain, but not an overall increase in the number of GFAP expressing cells as in humans. However, additional research is needed to determine if the area occupied by GFAP immunoreactivity increases with age in chimpanzees.

Microglial activation and density increase with age in the human neocortex, including in the hippocampal formation, entorhinal

TABLE 6 Independent samples *t*-test and one-way ANOVA statistics for chimpanzees with mild to severe astrogliosis and with and without Aβ-ir plaques, Aβ-ir vessels, severe CAA, NFT, and tau NC

		Aβ PLAQUES			Aβ VESSELS/CAA		
	Subregion/Morphology	*t*	*df*	*p*	*F*	*df*	*p*
GFAP-ir Av	Layer I	−.40	20	.69	2.68	2, 19	.09
	Layer III	−.07	20	.95	.21	2, 19	.81
	WM	.21	20	.84	.30	2, 19	.74
GFAP-ir SV	Layer I	−.27	20	.79	1.60	2, 19	.23
	Layer III	−.11	20	.91	1.24	2, 19	.31
	WM	−.94	20	.36	2.40	2, 19	.12
Iba1-ir Mv (Layer III)	Total	1.17	20	.26	4.06	2, 19	.03
	Ramified	1.87	16	.09	10.97	2, 15	.00**
	Intermediate	.29	18	.78	.23	2, 17	.80
	Amoeboid	.44	18	.66	2.16	2, 17	.15
Nissl (Layer III)	Nv	.20	20	.85	.48	2, 19	.63
	Gv	−.43	20	.67	.26	2, 19	.78
	G:N	−.90	20	.38	.70	2, 19	.93
		NFT			TAU NC		
	Subregion/Morphology	*t*	*df*	*p*	*t*	*df*	*p*
GFAP-ir Av	Layer I	−1.05	20	.31	.39	20	.70
	Layer III	−.21	20	.84	−.79	20	.44
	WM	.21	20	.84	1.23	20	.23
GFAP-ir SV	Layer I	.07	20	.94	.39	20	.70
	Layer III	.26	20	.80	.48	20	.63
	WM	−.73	5	.50	−.40	5	.70
Iba1-ir Mv (Layer III)	Total	.11	20	.92	1.60	20	.13
	Ramified	1.95	15	.23	2.04	13	.06
	Intermediate	−.07	18	.95	.47	18	.64
	Amoeboid	−.36	18	.72	.16	18	.88
Nissl (Layer III)	Nv	1.38	20	.18	−1.40	20	.18
	Gv	.30	20	.77	−3.03	20	.01*
	G:N	−1.09	20	.29	−2.25	20	.04

Abbreviations: Aβ, amyloid-beta; CAA, cerebral amyloid angiopathy; NC, neuritic cluster; NFT, neurofibrillary tangle.

*denotes significance with a Bonferroni correction for multiple comparison testing with $\alpha \leq .02$ for Av, SV, Nv, Gv, G:N, and $\alpha \leq .01$ for Mv for t-tests; **denotes significance with a Bonferroni correction with $\alpha = .05$ for one-way ANOVA tests.

cortex, and WM (DiPatre & Gelman, 1997; Gefen et al., 2019; Pelvig et al., 2008). Rhesus and pig-tailed macaques also display age-related increases in neocortical WM microglial densities (Robillard et al., 2016; Shobin et al., 2017). Our original analysis in chimpanzees revealed that age was not associated with greater Mv or morphological changes in the DLPFC, temporal cortex, or hippocampus (Edler et al., 2018). However, diverging from our prior report, the current investigation found that the number of ramified microglia significantly decreased, while amoeboid Mv increased with aging in layer III of the chimpanzee DLPFC. The distinct findings are clearly due to the inclusion of younger animals in this study (n = 12, 12–27 years; Figure 5c,d), as our original research included only aged individuals (n = 20, 37–62 years). Similarly, while microglia numbers did not vary with age in the hippocampus of marmosets, decreased numbers of ramified microglia were noted (Rodriguez-Callejas et al., 2016). Microglia density also was not affected by age in the visual cortex or midbrain of rhesus monkeys (Kanaan et al., 2010; Peters et al., 2008; Rodriguez-Callejas et al., 2016). These data indicate that brain regions are differentially impacted by neuroinflammation during the aging process in nonhuman primates and differ from elderly humans. Furthermore, chimpanzees experience a shift from higher numbers of ramified to amoeboid microglia during aging, signifying an increase in activation and a greater need for phagocytosis which may be related to the age-associated increase in Aβ we observed previously (Edler et al., 2017; Kettenmann et al., 2011). In contrast to what has been observed in humans, age was not associated with increased

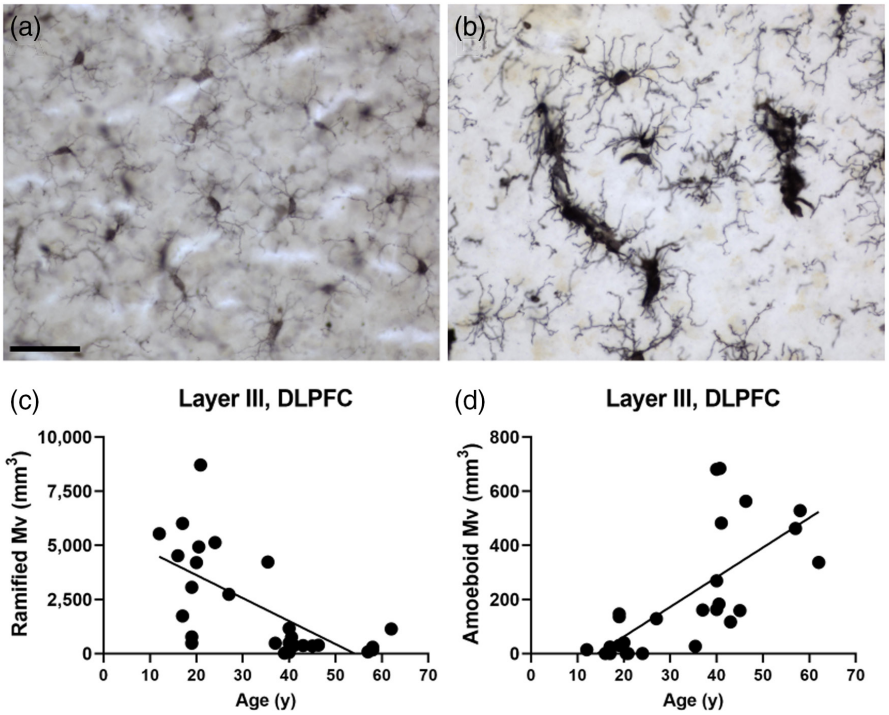

FIGURE 5 Photomicrographs of Iba1-ir microglia in DLPFC layer III of a young (a, female, 16 y) and an aged (b, female, 51 y) chimpanzee. With aging, ramified Mv (c) decrease, while amoeboid Mv increase in the chimpanzee brain (d). Iba1, ionized calcium-binding adaptor 1, DLPFC, dorsolateral prefrontal cortex, Mv, microglia density. Scale bar: a–b, 25 μm.

microglial proliferation in the chimpanzee neocortex or hippocampus, suggesting they do not experience the full "primed" phenotype associated with aging in humans. Whether this affords the chimpanzee protection from the neurodegenerative processes and cognitive impairments noted in AD remains to be determined.

Besides aging, astrocyte and microglia activation are commonly found in response to both amyloid and tau pathology in humans, although regional variations have been noted (Armstrong, 2009; Beach et al., 1989; Ekonomou et al., 2015; Heneka et al., 2010). Specifically, in individuals with AD, microglia and astrocyte area densities were significantly greater in the midtemporal gyrus (MTG) (Hoozemans et al., 2011). Moreover, astrocyte densities positively correlated with senile neuritic Aβ plaques and NFT in the temporal lobe, and increased microglial density and proliferation occurs concomitant with Aβ plaques and NFT in the hippocampus (Ekonomou et al., 2015; Harpin et al., 1990; Marlatt et al., 2014; McGeer et al., 1987; Simpson et al., 2010; Streit et al., 2009). While an abundance of research supports the concept that Aβ initiates microglial activation, a study examining four humans with substantial plaque loads in the absence of tau lesions found no evidence of microglial activation in the temporal cortex (Streit et al., 2009). In addition, microglia density in postmortem AD brains increased linearly, even after Aβ burden stopped increasing, and correlated with NFT burden instead of plaque load (Streit et al., 2009). However, fluctuations in astrocytes and microglia may be regionally specific. For example, GFAP mRNA expression was positively correlated with senile plaque density in the temporal cortex, but not in the frontal cortex, of nondemented versus AD individuals (Prince et al., 1993). Furthermore, cognitive function was inversely associated with GFAP in the occipital, parietal, and temporal lobes, but not in the frontal lobe of AD individuals (Kashon et al., 2004).

Systematic studies of neuroinflammatory markers in association with AD pathology in nonhuman primates are incredibly rare, although reactive astrocytes and activated microglia have been reported adjacent to Aβ and tau lesions in marmosets, macaques, gorillas, and chimpanzees (Edler et al., 2018; Härtig et al., 1997; Martin et al., 1994; Munger et al., 2019; Perez et al., 2013; Rodriguez-Callejas et al., 2016; Schultz et al., 2000). Tau-positive microglia and astrocytes also have been observed in the brains of marmosets, hamadryas baboons, mountain gorillas, and chimpanzees (Edler et al., 2018; Perez et al., 2013; Rodriguez-Callejas et al., 2016; Schultz et al., 2000). In our prior analyses of aged chimpanzees (n = 20, 37–62 years), we found that GFAP-ir Av (layer I) was positively correlated with Aβ-ir vessel volume and tau NC density, while Mv, Gv, and G:N ratio (layer III) were not associated with AD lesions in the DLPFC of chimpanzees (Edler et al., 2018, 2020; Munger et al., 2019). In contrast, our current analyses found that chimpanzees with Aβ-ir vessels displayed significantly decreased GFAP-ir Av (layer I, WM), compared to those lacking AD-like lesions (Tables 4 and 5, Figure 4). In addition, chimpanzees with NFT had reduced ramified Mv, while those with tau NC had greater overall Gv and G:N ratios. The discrepancies are due to multiple factors. In the initial studies, we performed regression analyses using cell densities (e.g., Av, Mv) with pathology volumes (Aβ-ir plaque and vessels) or densities (NFT, tau NC). In the present investigation, we categorized chimpanzees into groups based on the presence or

absence of pathologic lesion and performed ANOVAs (Table 1). We also increased our resolution by quantifying stereological data in 11 additional young chimpanzees (12–27 years), of which nine lacked AD lesions and served as a control group. Furthermore, our initial reports did not separate apes with severe CAA from those with mild or moderate CAA, like we did in this report. When apes with severe CAA are removed from the original analyses conducted in Munger et al. (2019), the increase in GFAP-ir Av correlated with Aβ-ir vessel volume changes to a decreasing trend in GFAP-ir Av, like the one observed in Figure 4a. These results suggest that mild to moderate CAA in chimpanzees is associated with decreased GFAP-ir Av in layer I of the DLPFC, while severe CAA likely results in significant astrogliosis. Likewise, in the original manuscript, one of the apes with severe CAA had the highest tau NC density and was a pathologic outlier, while two of the younger chimpanzees with extreme astrogliosis in this study had tau NC, which resulted in a lack of significant differences in GFAP-ir Av regardless of the absence or presence of tau lesions in this analysis. Finally, a significant decrease in ramified Mv in the presence of Aβ-ir plaques and vessels, severe CAA, and NFT was noted (Figure 4d), as well as a decrease in total Mv (Figure 4c) and an increase in amoeboid Mv (Figure 4e) in apes with Aβ-ir vessels. These findings indicate a decrease in the number of resting microglia and an increase in activated, phagocytotic microglia in these apes, which is similarly observed in AD. However, chimpanzees do not experience an overall increase in Av and Mv in association with plaques and NFT like humans with AD. Interestingly, we did not detect changes in Av or total Mv during aging, indicating these may be a potentially unique response to Aβ deposition in blood vessels. Another explanation for the decreased glial activation with vascular amyloid may be that our control group of chimpanzees lacked AD pathology but generally had greater levels of astrogliosis ($n = 4$ extreme, 2 severe, 2 moderate, 1 mild), and therefore, higher Av and Mv typically. The shift of reduced ramified Mv in chimpanzees with Aβ-ir vessels and NFT signifies mildly increased levels of microglial activation, while the absence of change in Av with AD pathology is a noteworthy difference from humans that warrants further investigation. Unexpectedly, total Gv and G:N ratio were higher in chimpanzees with tau NC. As tau NC was not correlated with greater Av and Mv, this finding implicates a possible increase in oligodendrocytes. Tau is present naturally in the soma and processes of oligodendrocytes, and tau-immunoreactive oligodendrocytes have been confirmed in baboons and humans (LoPresti et al., 1995; Nishimura et al., 1995; Schultz et al., 2000). In addition, evidence has shown that the seeding and spreading of human tau occurs in oligodendrocytes but not astrocytes (Ferrer et al., 2019). However, additional analyses are required to determine if the increase in Gv and G:N ratio with tau NC is associated with greater oligodendrocyte numbers in the chimpanzee brain.

Like our previous report, GFAP-ir astrocytes in layer I are more densely packed compared to those in layer III and WM of the chimpanzee DLPFC (Munger et al., 2019). Layer I and III astrocytes, both interlaminar and protoplasmic, have a greater SV compared to WM fibrous astrocytes, highlighting the importance of these astrocytes, especially interlaminar astrocytes, in regulating neuronal activity. Astrocytes have an important role in maintaining appropriate neuronal communication (Araque et al., 1999; Diniz et al., 2014; Perea et al., 2009; Rothstein et al., 1994, 1996), being involved in the regulation, maintenance, pruning, and remodeling of synapses (Chung et al., 2013, 2015; Diniz et al., 2014). Astrocytes are also the primary cell responsible for the rapid reuptake of the excitatory neurotransmitter glutamate, thus preventing excitotoxicity (Lehre et al., 1998; Sulkowski et al., 2014). Astrocytes mainly participate in the tripartite synapse which allows them unique access to pre- and postsynaptic neurons, giving them the ability to maintain bidirectional communication (Araque et al., 1999). The human protoplasmic astrocyte has a 2.6-fold increased diameter, 16.5-fold increase in volume, and 10-fold increase in the number of processes compared to rodents (Oberheim et al., 2009). The increase in size of the astrocyte and its encompassing domain allows an individual human protoplasmic astrocyte to contact, and therefore, potentially modulate approximately 270,000 to 2 million neuronal synapses compared to only 20,000 to 120,000 for rodents (Bushong et al., 2002; Oberheim et al., 2009). The observation that chimpanzees possess an increased interlaminar Av and increased gray matter astrocyte SV emphasizes the importance of these cells in maintaining proper neuronal function and communication.

In conclusion, we describe an extreme form of astrogliosis indicative of global CNS inflammation in chimpanzees, characterized by extensive GFAP upregulation, increased astrocyte density, and complete loss of domain organization and the interlaminar palisade in the absence of significant microglial activation and AD lesions. Aging in the chimpanzee brain is associated with morphological variations in microglia, but not with changes in overall density changes in microglia or astrocytes. In contrast, AD lesions correlate with variations in microglia, astrocyte, and overall glia densities. Further work is needed to determine if the age- and pathology-related differences in neuroinflammatory response between humans and chimpanzees are protective.

DECLARATION OF TRANSPARENCY

The authors, reviewers and editors affirm that in accordance to the policies set by the *Journal of Neuroscience Research*, this manuscript presents an accurate and transparent account of the study being reported and that all critical details describing the methods and results are present.

AUTHOR CONTRIBUTIONS

Melissa K. Edler: conceptualization (equal); formal analysis (equal); investigation (equal); methodology (equal); visualization (equal); writing – original draft preparation (equal); writing – review and editing (equal). **Emily L. Munger**: conceptualization (equal); formal analysis (equal); investigation (equal); methodology (equal); visualization (equal); writing – original draft preparation (equal); writing – review and editing (equal). **Hannah Maycon**: visualization (supporting); writing – review and editing (supporting). **William D. Hopkins**: resources (equal); writing – review and editing (supporting). **Patrick**

R. Hof: resources (equal); writing – review and editing (supporting). **Chet C. Sherwood**: resources (equal); writing – review and editing (supporting). **Mary Ann Raghanti**: conceptualization (equal); formal analysis (supporting); funding acquisition; project administration; supervision; writing – review and editing (supporting).

ACKNOWLEDGMENTS

This research was funded by the National Institutes of Health (NIH 3U42OD011197-19S1, WDH and MAR; NIH R01AG067419-01A1, WDH, MAR, MKE, and CCS) and the National Science Foundation (NSF BCS-1846201). We thank Dr. Richard S. Meindl for statistical advice. We are grateful to each of the following for the use of brain materials: The National Chimpanzee Brain Resource (NIH grant NS092988), NINDS grants NS-402867 and NS0-73134, The Great Ape Aging Project (supported by NIH grant AG014308), and the NIH NeuroBioBank (human brains).

FUNDING INFORMATION

Grant sponsors: National Institutes of Health; Grant number: R01AG067419 (WDH, MKE, MAR, CCS), NIH 3U42OD011197-19S1 (WDH and MAR). National Science Foundation; Grant number: NSF BCS-1846201 (MAR).

CONFLICT OF INTEREST

The authors declare no competing interests.

PEER REVIEW

The peer review history for this article is available at https://publons.com/publon/10.1002/jnr.25167.

DATA AVAILABILITY STATEMENT

Upon publication, data will be available on the National Chimpanzee Brain Resource website: http://chimpanzeebrain.org.

ORCID

Melissa K. Edler https://orcid.org/0000-0002-9084-9539
Emily L. Munger https://orcid.org/0000-0001-7437-2032
William D. Hopkins https://orcid.org/0000-0003-3480-1853
Patrick R. Hof https://orcid.org/0000-0002-3208-1154
Chet C. Sherwood https://orcid.org/0000-0001-6711-449X
Mary Ann Raghanti https://orcid.org/0000-0002-6842-1907

REFERENCES

Allen, J. S., Bruss, J., Brown, C. K., & Damasio, H. (2005). Normal neuroanatomical variation due to age: The major lobes and a parcellation of the temporal region. *Neurobiology of Aging*, *26*, 1245–1260.

Araque, A., Parpura, V., Sanzgiri, R. P., & Haydon, P. G. (1999). Tripartite synapses: Glia, the unacknowledged partner. *Trends in Neurosciences*, *22*, 208–215.

Armstrong, R. A. (2009). The molecular biology of senile plaques and neurofibrillary tangles in Alzheimer's disease. *Folia Neuropathologica*, *47*, 289–299.

Autrey, M. M., Reamer, L. A., Mareno, M. C., Sherwood, C. C., Herndon, J. G., Preuss, T., Schapiro, S. J., & Hopkins, W. D. (2014). Age-related effects in the neocortical organization of chimpanzees: Gray and white matter volume, cortical thickness, and gyrification. *NeuroImage*, *101*, 59–67.

Bauer, R., & Fuster, J. (1976). Delayed-matching and delayed-response deficit from cooling dorsolateral prefrontal cortex in monkeys. *Journal of Comparative and Physiological Psychology*, *90*, 293–302.

Beach, T. G., Walker, R., & McGeer, E. G. (1989). Patterns of gliosis in Alzheimer's disease and aging cerebrum. *Glia*, *2*, 420–436.

Brickman, A. M., Habeck, C., Zarahn, E., Flynn, J., & Stern, Y. (2007). Structural MRI covariance patterns associated with normal aging and neuropsychological functioning. *Neurobiology of Aging*, *28*, 284–295.

Bushong, E., Martone, M., Jones, Y., & Ellisman, M. (2002). Protoplasmic astrocytes in CA1 stratum radiatum occupy separate anatomical domains. *The Journal of Neuroscience*, *22*, 183–192.

Cargill, R., Kohama, S. G., Struve, J., Su, W., Banine, F., Witkowski, E., Back, S. A., & Sherman, L. S. (2012). Astrocytes in aged nonhuman primate brain gray matter synthesize excess hyaluronan. *Neurobiology of Aging*, *33*, 830.e13–830.e24.

Che-Castaldo, J., Havercamp, K., Watanuki, K., Matsuzawa, T., Hirata, S., & Ross, S. R. (2021). Comparative survival analyses among captive chimpanzees (*Pan troglodytes*) in America and Japan. *PeerJ*, *9*, e11913. https://pubmed.ncbi.nlm.nih.gov/34447626

Chen, J., Buchanan, J. B., Sparkman, N. L., Godbout, J. P., Freund, G. G., & Johnson, R. W. (2008). Neuroinflammation and disruption in working memory in aged mice after acute stimulation of the peripheral innate immune system. *Brain, Behavior, and Immunity*, *22*, 301–311.

Chung, W. S., Allen, N. J., & Eroglu, C. (2015). Astrocytes control synapse formation, function, and elimination. *Cold Spring Harbor Perspectives in Biology*, *7*, a020370.

Chung, W. S., Clarke, L. E., Wang, G. X., Stafford, B. K., Sher, A., Chakraborty, C., Joung, J., Foo, L. C., Thompson, A., Chen, C., Smith, S. J., & Barres, B. A. (2013). Astrocytes mediate synapse elimination through MEGF10 and MERTK pathways. *Nature*, *504*, 394–400.

Colombo, J. A., Quinn, B., & Puissant, V. (2002). Disruption of astroglial interlaminar processes in Alzheimer's disease. *Brain Research Bulletin*, *58*, 235–242.

Colombo, J. A., Sherwood, C. C., & Hof, P. R. (2004). Interlaminar astroglial processes in the cerebral cortex of great apes. *Anatomy and Embryology*, *208*, 215–218.

Cotrina, M. L., & Nedergaard, M. (2002). Astrocytes in the aging brain. *Journal of Neuroscience Research*, *67*, 1–10.

Dall'Olio, F., Vanhooren, V., Chen, C. C., Slagboom, P. E., Wuhrer, M., & Franceschi, C. (2013). N-glycomic biomarkers of biological aging and longevity: A link with inflammaging. *Aging Research Reviews*, *12*, 685–698.

David, J. P., Ghozali, F., Fallet-Bianco, C., Wattez, A., Delaine, S., Boniface, B., di Menza, C., & Delacourte, A. (1997). Glial reaction in the hippocampal formation is highly correlated with aging in human brain. *Neuroscience Letters*, *235*, 53–56.

Demers, M., Suidan, G. L., Andrews, N., Martinod, K., Cabral, J. E., & Wagner, D. D. (2018). Solid peripheral tumor leads to systemic inflammation, astrocyte activation and signs of behavioral despair in mice. *PLoS One*, *13*, 1–14.

Diniz, L. P., Matias, I. C. P., Garcia, M. N., & Gomes, F. C. A. (2014). Astrocytic control of neural circuit formation: Highlights on TGF-β signaling. *Neurochemistry International*, *78*, 18–27.

DiPatre, P. L., & Gelman, B. B. (1997). Microglial cell activation in aging and Alzheimer disease: Partial linkage with neurofibrillary tangle burden in the hippocampus. *Journal of Neuropathology and Experimental Neurology*, *56*, 143–149.

Edler, M. K., Munger, E. L., Meindl, R. S., Hopkins, W. D., Ely, J. J., Erwin, J. M., Mufson, E. J., Hof, P. R., Sherwood, C. C., & Raghanti, M. A. (2020). Neuron loss associated with age but not Alzheimer's disease pathology in the chimpanzee brain. *Philosophical Transactions of the Royal Society, B: Biological Sciences*, *375*, 1–10.

Edler, M. K., Sherwood, C. C., Meindl, R. S., Hopkins, W. D., Ely, J. J., Erwin, J. M., Mufson, E. J., Hof, P. R., & Raghanti, M. A. (2017). Aged chimpanzees exhibit pathologic hallmarks of Alzheimer's disease. *Neurobiology of Aging*, *59*, 107–120. https://doi.org/10.1016/j.neurobiolaging.2017.07.006

Edler, M. K., Sherwood, C. C., Meindl, R. S., Munger, E. L., Hopkins, W. D., Ely, J. J., Erwin, J. M., Perl, D. P., Mufson, E. J., Hof, P. R., & Raghanti, M. A. (2018). Microglia changes associated to Alzheimer's disease pathology in aged chimpanzees. *Journal of Comparative Neurology*, *526*, 2921–2936.

Ekonomou, A., Savva, G. M., Brayne, C., Forster, G., Francis, P. T., Johnson, M., Perry, E. K., Attems, J., Somani, A., Minger, S. L., Ballard, C. G., & Medical Research Council Cognitive Function and Ageing Neuropathology Study. (2015). Stage-specific changes in neurogenic and glial markers in Alzheimer's disease. *Biological Psychiatry*, *77*, 711–719. https://doi.org/10.1016/j.biopsych.2014.05.021

Ferrer, I., Aguiló García, M., Carmona, M., Andrés-Benito, P., Torrejón-Escribano, B., Garcia-Esparcia, P., & del Rio, J. (2019). Involvement of oligodendrocytes in tau seeding and spreading in tauopathies. *Frontiers in Aging Neuroscience*, *11*, 112. https://www.frontiersin.org/article/10.3389/fnagi.2019.00112

Finch, C., Morgan, T., Rozovsky, I., Xie, Z., Weindruch, R., & Prolla, T. (2002). Microglia and aging in the brain. In W. Streit (Ed.), *Microglia in the regenerating and degenerating central nervous system*. Springer-Verlag.

Finch, C. E. (2003). Neurons, glia, and plasticity in normal brain aging. *Neurobiology of Aging*, *24*, 123–127.

Foley, J. E., Rand, C., & Leutenegger, C. (2003). Inflammation and changes in cytokine levels in neurological feline infectious peritonitis. *Journal of Feline Medicine and Surgery*, *5*, 313–322. https://pubmed.ncbi.nlm.nih.gov/14623200

Franceschi, C., Bonafè, M., Valensin, S., Olivieri, F., De Luca, M., Ottaviani, E., et al. (2000). Inflamm-aging. An evolutionary perspective on immunosenescence. *Annals of the New York Academy of Sciences*, *908*, 244–254.

Franceschi, C., Valensin, S., Bonafè, M., Paolisso, G., Yashin, A. I., Monti, D., & de Benedictis, G. (2000). The network and the remodeling theories of aging: Historical background and new perspectives. *Experimental Gerontology*, *35*, 879–896.

Fuster, J., & Alexander, G. (1971). Neuron activity related to short-term memory. *Science*, *173*, 652–654.

Gefen, T., Kim, G., Bolbolan, K., Geoly, A., Ohm, D., Oboudiyat, C., Shahidehpour, R., Rademaker, A., Weintraub, S., Bigio, E. H., Mesulam, M. M., Rogalski, E., & Geula, C. (2019). Activated microglia in cortical white matter across cognitive aging trajectories. *Frontiers in Aging Neuroscience*, *11*, 94.

Geula, C., Wu, C. K., Saroff, D., Lorenzo, A., Yuan, M., & Yankner, B. A. (1998). Aging renders the brain vulnerable to amyloid beta-protein neurotoxicity. *Nature Medicine*, *4*, 827–831.

Goedert, M., Jakes, R., Spillantini, M. G., Crowther, R. A., Cohen, P., Vanmechelen, E., Probst, A., Götz, J., & Bürki, K. (1995). Tau protein in Alzheimer's disease. *Biochemical Society Transactions*, *23*, 80–85.

Goss, J., Finch, C., & Morgan, D. (1991). Age-related changes in glial fibrillary acidic protein mRNA in the mouse brain. *Neurobiology of Aging*, *12*, 165–170.

Haley, G. E., Kohama, S. G., Urbanski, H. F., & Raber, J. (2010). Age-related decreases in SYN levels associated with increases in MAP-2, apoE, and GFAP levels in the rhesus macaque prefrontal cortex and hippocampus. *Age (Omaha)*, *32*, 283–296.

Harman, D. (1956). Aging: A theory based on free radical and radiation chemistry. *Journal of Gerontology*, *11*, 298–300.

Harpin, M. L., Delaère, P., Javoy-Agid, F., Bock, E., Jacque, C., Delpech, B., Villarroya, H., Duyckaerts, C., Hauw, J. J., & Baumann, N. (1990). Glial fibrillary acidic protein and βA4 protein deposits in temporal lobe of aging brain and senile dementia of the Alzheimer type: Relation with the cognitive state and with quantitative studies of senile plaques and neurofibrillary tangles. *Journal of Neuroscience Research*, *27*, 587–594. https://doi.org/10.1002/jnr.490270420

Härtig, W., Brückner, G., Schmidt, C., Brauer, K., Bodewitz, G., Turner, J. D., & Bigl, V. (1997). Co-localization of β-amyloid peptides, apolipoprotein E and glial markers in senile plaques in the prefrontal cortex of old rhesus monkeys. *Brain Research*, *751*, 315–322.

Heneka, M. T., O'Banion, M. K., Terwel, D., & Kummer, M. P. (2010). Neuroinflammatory processes in Alzheimer's disease. *Journal of Neural Transmission*, *117*, 919–947.

Henry, C. J., Huang, Y., Wynne, A. M., & Godbout, J. P. (2009). Peripheral lipopolysaccharide (LPS) challenge promotes microglial hyperactivity in aged mice that is associated with exaggerated induction of both pro-inflammatory IL-1beta and anti-inflammatory IL-10 cytokines. *Brain, Behavior, and Immunity*, *23*, 309–317.

Hoozemans, J. J. M., Rozemuller, A. J. M., van Haastert, E. S., Eikelenboom, P., & van Gool, W. A. (2011). Neuroinflammation in Alzheimer's disease wanes with age. *Journal of Neuroinflammation*, *8*, 171. https://pubmed.ncbi.nlm.nih.gov/22152162

Imai, Y., Ibata, I., Ito, D., Ohsawa, K., & Kohsaka, S. (1996). A novel gene iba1 in the major histocompatibility complex class III region encoding an EF hand protein expressed in a monocytic lineage. *Biochemical and Biophysical Research Communications*, *224*, 855–862.

Iwashyna, T. J., Ely, E. W., Smith, D. M., & Langa, K. M. (2010). Long-term cognitive impairment and functional disability among survivors of severe sepsis. *Journal of the American Medical Association*, *304*, 1787–1794.

Janota, C. S., Brites, D., Lemere, C. A., & Brito, M. A. (2015). Glio-vascular changes during ageing in wild-type and Alzheimer's disease-like APP/PS1 mice. *Brain Research*, *1620*, 153–168.

Kanaan, N. M., Kordower, J. H., & Collier, T. J. (2010). Age-related changes in glial cells of dopamine midbrain subregions in rhesus monkeys. *Neurobiology of Aging*, *31*, 937–952. https://doi.org/10.1016/j.neurobiolaging.2008.07.006

Kane, M. J., & Engle, R. W. (2002). The role of prefrontal cortex in working-memory capacity, executive attention, and general T. Wynn, F Coolidge. *Journal of Human Evolution*, *46*, 341–365.

Kashon, M. L., Ross, G. W., O'Callaghan, J. P., Miller, D. B., Petrovitch, H., Burchfiel, C. M., et al. (2004). Associations of cortical astrogliosis with cognitive performance and dementia status. *Journal of Alzheimer's Disease*, *6*, 595–604.

Kettenmann, H., Hanisch, U.-K., Noda, M., & Verkhratsky, A. (2011). Physiology of microglia. *Physiological Reviews*, *91*, 461–553.

Kim, K. S., Miller, D. L., Sapienza, V. J., Chen, C. M. J., Bai, C., Grundke-Iqbal, I., Currie, J. R., & Wisniewski, H. M. (1988). Production and characterization of monoclonal antibodies reactive to synthetic cerebrovascular amyloid peptide. *Neuroscience Research Communications*, *2*, 121–130.

Kubota, K., & Niki, H. (1971). Prefrontal cortical unit activity and delayed alternation performance in monkeys. *Journal of Neurophysiology*, *34*, 337–347.

Landfield, P. W., Rose, G., Sandles, L., Wohstaddter, T. C., & Lynch, G. (1977). Patterns of astroglial hypertrophy and neuronal degeneration in the hippocampus of aged, memory-deficient rats. *Journal of Gerontology*, *32*, 3–12.

Lehre, P., Yallapu, M. M., Sari, Y., Fisher, P. B., & Kumar, S. (1998). The number of glutamate transporter subtype molecules at glutamatergic synapses: Chemical and stereological quantification in young adult rat brain. *Journal of Neuroscience*, *18*, 8751–8757.

Leung, E., Guo, L., Bu, J., Maloof, M., El Khoury, J., & Geula, C. (2011). Microglia activation mediates fibrillar amyloid-β toxicity in the aged primate cortex. *Neurobiology of Aging*, *32*, 387–397.

LoPresti, P., Szuchet, S., Papasozomenos, S. C., Zinkowski, R. P., & Binder, L. I. (1995). Functional implications for the microtubule-associated protein tau: Localization in oligodendrocytes.

Proceedings of the National Academy of Sciences of the United States of America, *92*, 10369–10373. https://doi.org/10.1073/pnas.92.22.10369

Marlatt, M. W., Bauer, J., Aronica, E., van Haastert, E. S., Hoozemans, J. J. M., Joels, M., & Lucassen, P. J. (2014). Proliferation in the Alzheimer hippocampus is due to microglia, not astroglia, and occurs at sites of amyloid deposition. *Neural Plasticity*, *2014*, 1–12.

Martin, L. J., Pardo, C. A., Cork, L. C., & Price, D. L. (1994). Synaptic pathology and glial responses to neuronal injury precede the formation of senile plaques and amyloid deposits in the aging cerebral cortex. *American Journal of Pathology*, *145*, 1358–1381.

McGeer, P. L., Itagaki, S., Tago, H., & McGeer, E. G. (1987). Reactive microglia in patients with senile dementia of the Alzheimer type are positive for the histocompatibility glycoprotein HLA-DR. *Neuroscience Letters*, *79*, 195–200.

Mesquita, L. P., Hora, A. S., de Siqueira, A., Salvagni, F. A., Brandão, P. E., & Maiorka, P. C. (2016). Glial response in the central nervous system of cats with feline infectious peritonitis. *Journal of Feline Medicine and Surgery*, *18*, 1023–1030.

Miller, M., & Orbach, J. (1972). Retention of spatial alternation following frontal lobe resections in stump-tailed-macaques. *Neuropsychologia*, *10*, 291–298.

Moller, P., Lohr, M., Folkmann, J. K., Mikkelsen, L., & Loft, S. (2010). Aging and oxidatively damaged nuclear DNA in animal organs. *Free Radical Biology & Medicine*, *48*, 1275–1285.

Montine, T. J., Phelps, C. H., Beach, T. G., Bigio, E. H., Cairns, N. J., Dickson, D. W., Duyckaerts, C., Frosch, M. P., Masliah, E., Mirra, S. S., Nelson, P. T., Schneider, J. A., Thal, D. R., Trojanowski, J. Q., Vinters, H. V., Hyman, B. T., National Institute on Aging, & Alzheimer's Association. (2012). National Institute on Aging-Alzheimer's Association guidelines for the neuropathologic assessment of Alzheimer's disease: A practical approach. *Acta Neuropathologica*, *123*, 1–11. http://www.pubmedcentral.nih.gov/articlerender.fcgi?artid=3268003&tool=pmcentrez&rendertype=abstract

Morgan, T., Rozovsky, I., Goldsmith, S., Stone, D., Yoshida, T., & Finch, C. (1997). Increased transcription of the astrocyte gene GFAP during middle-age is attenuated by food restriction: Implications for the role of oxidative stress. *Free Radical Biology & Medicine*, *23*, 524–528.

Munger, E. L., Edler, M. K., Hopkins, W. D., Ely, J. J., Erwin, J. M., Perl, D. P., Mufson, E. J., Hof, P. R., Sherwood, C. C., & Raghanti, M. A. (2019). Astrocytic changes with aging and Alzheimer's disease-type pathology in chimpanzees. *Journal of Comparative Neurology*, *527*, 1179–1195.

Nichols, N. R., Day, J. R., Laping, N. J., Johnson, S. A., & Finch, C. E. (1993). GFAP mRNA increases with age in rat and human brain. *Neurobiology of Aging*, *14*, 421–429.

Nishimura, M., Tomimoto, H., Suenaga, T., Namba, Y., Ikeda, K., Akiguchi, I., et al. (1995). Immunocytochemical characterization of glial fibrillary tangles in Alzheimer's disease brain. *American Journal of Pathology*, *146*, 1052–1058. https://pubmed.ncbi.nlm.nih.gov/7747799

Oberheim, N. A., Takano, T., Han, X., He, W., Lin, J. H. C., Wang, F., Xu, Q., Wyatt, J. D., Pilcher, W., Ojemann, J. G., Ransom, B. R., Goldman, S. A., & Nedergaard, M. (2009). Uniquely hominid features of adult human astrocytes. *The Journal of Neuroscience*, *29*, 3276–3287.

O'Callaghan, N. R., & Miller, D. B. (1991). The concentration of glial fibrillary acidic protein increases with age in the mouse and rat brain. *Neurobiology of Aging*, *12*, 392–399.

Pekny, M., Wilhelmsson, U., & Pekna, M. (2014). The dual role of astrocyte activation and reactive gliosis. *Neuroscience Letters*, *565*, 30–38, 38. https://doi.org/10.1016/j.neulet.2013.12.071

Pelvig, D. P., Pakkenberg, H., Stark, A. K., & Pakkenberg, B. (2008). Neocortical glial cell numbers in human brains. *Neurobiology of Aging*, *29*, 1754–1762. http://www.ncbi.nlm.nih.gov/pubmed/17544173

Perea, G., Navarrete, M., & Araque, A. (2009). Tripartite synapses: Astrocytes process and control synaptic information. *Trends in Neurosciences*, *32*, 421–431.

Perez, S. E., Raghanti, M. A., Hof, P. R., Kramer, L., Ikonomovic, M. D., Lacor, P. N., Erwin, J. M., Sherwood, C. C., & Mufson, E. J. (2013). Alzheimer's disease pathology in the neocortex and hippocampus of the western lowland gorilla (Gorilla gorilla gorilla). *Journal of Comparative Neurology*, *521*, 4318–4338.

Perry, V. H., Newman, T. A., & Cunningham, C. (2004). The impact of systemic infection on the progression of neurodegenerative disease. *Nature Reviews. Neuroscience*, *4*, 103–112.

Peters, A., Sethares, C., & Moss, M. B. (2010). How the primate fornix is affected by age. *Bone*, *518*, 3962–3980.

Peters, A., Sethares, C., & Moss, M. B. (2011). How the primate fornix is affected by age. *The Journal of Comparative Neurology*, *518*, 3962–3980.

Peters, A., Verderosa, A., & Sethaers, C. (2008). The neuroglial population in the primary visual cortex of the aging rhesus monkey. *Glia*, *56*, 1151–1161.

Poon, H. F., Calabrese, V., Scapagnini, G., & Butterfield, D. A. (2004). Free radicals and brain aging. *Clinics in Geriatric Medicine*, *20*, 329–359.

Prince, G. I., Delaere, P., Fages, C., Duyckaerts, C., Hauw, J.-J., & Tardy, M. (1993). Alterations of glial fibrillary acidic protein mRNA level in the aging brain and in senile dementia of the Alzheimer type. *Neuroscience Letters*, *151*, 71–73. https://www.sciencedirect.com/science/article/pii/030439409390048P

Robillard, K. N., Lee, K. M., Chiu, K. B., & MacLean, A. G. (2016). Glial cell morphological and density changes through the lifespan of rhesus macaques. *Brain, Behavior, and Immunity*, *55*, 60–69. https://doi.org/10.1016/j.bbi.2016.01.006

Rodier, F., & Campisi, J. (2011). Four faces of cellular senescence. *Journal of Cell Biology*, *192*, 547–556.

Rodriguez-Callejas, J. D., Fuchs, E., Perez-Cruz, C., & Perez-Cruz, C. (2016). Evidence of tau hyperphosphorylation and dystrophic microglia in the common marmoset. *Frontiers in Aging Neuroscience*, *8*, 1–15.

Rosen, R. F., Farberg, A. S., Gearing, M., Dooyema, J., Long, P. M., Anderson, D. C., Davis-Turak, J., Coppola, G., Geschwind, D. H., Paré, J. F., Duong, T. Q., Hopkins, W. D., Preuss, T. M., & Walker, L. C. (2008). Tauopathy with paired helical filaments in an aged chimpanzee. *Jounral of Comparative Neurology*, *509*, 259–270.

Rothstein, J. D., Dykes-Hoberg, M., Pardo, C. A., Bristol, L. A., Jin, L., Kuncl, R. W., Kanai, Y., Hediger, M. A., Wang, Y., Schielke, J. P., & Welty, D. F. (1996). Knockout of glutamate transporters reveals a major role for astroglial transport in excitotoxicity and clearance of glutamate. *Neuron*, *16*, 675–686.

Rothstein, J. D., Martin, L., Levey, A. I., Dykes-Hoberg, M., Jin, L., Wu, D., Nash, N., & Kuncl, R. W. (1994). Localization of neuronal and glial glutamate transporters. *Neuron*, *13*, 713–725.

Schultz, C., Dehghani, F., Hubbard, G. B., Thal, D. R., Struckhoff, G., Braak, E., & Braak, H. (2000). Filamentous tau pathology in nerve cells, astrocytes, and oligodendrocytes of aged baboons. *Journal of Neuropathology and Experimental Neurology*, *59*, 39–52.

Serrano-Pozo, A., Frosch, M. P., Masliah, E., & Hyman, B. T. (2011). Neuropathological alterations in Alzheimer disease. *Cold Spring Harbor Perspectives in Medicine*, *1*, a006189. https://www.ncbi.nlm.nih.gov/pubmed/22229116

Sheffield, L. G., & Berman, N. E. J. (1998). Microglial expression of MHC class II increases in normal aging of nonhuman primates. *Neurobiology of Aging*, *19*, 47–55.

Sherwood, C., Gordon, A., Allen, J., Phillips, K., Hof, P., & Hopkins, W. (2011). Aging of the cerebral cortex differs between humans and chimpanzees. *Proceedings of the National Academy of Sciences of the United States of America*, *108*, 13029–13034.

Shobin, E., Bowley, M. P., Estrada, L. I., Heyworth, N. C., Orczykowski, M. E., Eldridge, S. A., Calderazzo, S. M., Mortazavi, F., Moore, T.

L., & Rosene, D. L. (2017). Microglia activation and phagocytosis: Relationship with aging and cognitive impairment in the rhesus monkey. *GeroScience*, *39*, 199–220.

Simpson, J. E., Ince, P. G., Lace, G., Forster, G., Shaw, P. J., Matthews, F., Savva, G., Brayne, C., Wharton, S. B., & MRC Cognitive Function and Ageing Neuropathology Study Group. (2010). Astrocyte phenotype in relation to Alzheimer-type pathology in the ageing brain. *Neurobiology of Aging*, *31*, 578–590. https://doi.org/10.1016/j.neurobiolaging.2008.05.015

Sloane, J. A., Hollander, W., Rosene, D. L., Moss, M. B., Kemper, T., & Abraham, C. R. (2000). Astrocytic hypertrophy and altered GFAP degradation with age in subcortical white matter of the rhesus monkey. *Brain Research*, *862*, 1–10.

Slomianka, L., & West, M. J. (2005). Estimators of the precision of stereological estimates: An example based on the CA1 pyramidal cell layer of rats. *Neuroscience*, *136*, 757–767.

Sofroniew, M. V. (2009). Molecular dissection of reactive astrogliosis and glial scar. *Trends in Neurosciences*, *32*, 638–647.

Sofroniew, M. V., & Vinters, H. V. (2010). Astrocytes: Biology and pathology. *Acta Neuropathologica*, *119*, 7–35.

Streit, W. J., Braak, H., Xue, Q. S., & Bechmann, I. (2009). Dystrophic (senescent) rather than activated microglial cells are associated with tau pathology and likely precede neurodegeneration in Alzheimer's disease. *Acta Neuropathologica*, *118*, 475–485.

Streit, W. J., Walter, S. A., & Pennell, N. A. (1999). Reactive microgliosis. *Progress in Neurobiology*, *57*, 563–581.

Sulkowski, G., Dabrowska-Bouta, B., Salinska, E., & Struzynska, L. (2014). Modulation of glutamate transport and receptor binding by glutamate receptor antagonists in EAE rat brain. *PLoS One*, *9*, e113954.

Terrando, N., Monaco, C., Ma, D., Foxwell, B. M., Feldmann, M., & Maze, M. (2010). Tumor necrosis factor-alpha triggers a cytokine cascade yielding postoperative cognitive decline. *Proceedings of the National Academy of Sciences of the United States of America*, *107*, 20518–20522.

Wood, B. M., Watts, D. P., Mitani, J. C., & Langergraber, K. E. (2017). Favorable ecological circumstances promote life expectancy in chimpanzees similar to that of human hunter-gatherers. *Journal of Human Evolution*, *105*, 41–56. https://www.sciencedirect.com/science/article/pii/S0047248417300052

Zimmerman, M. E., Brickman, A. M., Paul, R. H., Grieve, S. M., Tate, D. F., Gunstad, J., Cohen, R. A., Aloia, M. S., Williams, L. M., Clark, C. R., Whitford, T. J., & Gordon, E. (2006). The relationship between frontal gray matter volume and cognition varies across the healthy adult lifespan. *American Journal of Geriatric Psychiatry*, *14*, 823–833.

Zrzavy, T., Höftberger, R., Berger, T., Rauschka, H., Butovsky, O., Weiner, H., & Lassmann, H. (2019). Pro-inflammatory activation of microglia in the brain of patients with sepsis. *Neuropathology and Applied Neurobiology*, *45*, 278–290.

SUPPORTING INFORMATION

Additional supporting information can be found online in the Supporting Information section at the end of this article.

Transparent Science Questionnaire for Authors

How to cite this article: Edler, M. K., Munger, E. L., Maycon, H., Hopkins, W. D., Hof, P. R., Sherwood, C. C., & Raghanti, M. A. (2023). The association of astrogliosis and microglial activation with aging and Alzheimer's disease pathology in the chimpanzee brain. *Journal of Neuroscience Research*, *00*, 1–20. https://doi.org/10.1002/jnr.25167